University of South Bohemia

Faculty of Science

Department of Molecular Biology

Enzymes of Purine Salvage Pathway in *Trypanosoma brucei* and the Trypanocidal Action of Acyclic Nucleoside Phosphonates

Master thesis

Zuzana Kotrbová

Supervisor: RNDr. Alena Zíková, PhD.

České Budějovice, 2014

Kotrbová, Z., 2014: Enzymes of Purine Salvage Pathway in *Trypanosoma brucei* and the Trypanocidal Action of Acyclic Nucleoside Phosphonates. Mgr. Thesis in English – 57p., Faculty of Science, University of South Bohemia, České Budějovice, Czech Republic

Annotation:
This study aims to functionally characterize two enzymes, HGPRT and XPRT, of an essential purine salvage pathway in the infection stage of *Trypanosoma brucei*. Localization, *in vivo* function and *in vitro* activity of these enzymes were characterized. Effect of acyclic nucleoside phosphonates, putative inhibitors of HGXPRT, on the viability of bloodstream form of *T. brucei* was evaluated.

Prohlašuji, že svoji diplomovou práci jsem vypracovala samostatně pouze s použitím pramenů a literatury uvedených v seznamu citované literatury.

Prohlašuji, že v souladu s § 47b zákona č. 111/1998 Sb. v platném znění souhlasím se zveřejněním své diplomové práce, a to v nezkrácené podobě elektronickou cestou ve veřejně přístupné části databáze STAG provozované Jihočeskou univerzitou v Českých Budějovicích na jejích internetových stránkách, a to se zachováním mého autorského práva k odevzdanému textu této kvalifikační práce. Souhlasím dále s tím, aby toutéž elektronickou cestou byly v souladu s uvedeným ustanovením zákona č. 111/1998 Sb. zveřejněny posudky školitele a oponentů práce i záznam o průběhu a výsledku obhajoby kvalifikační práce. Rovněž souhlasím s porovnáním textu mé kvalifikační práce s databází kvalifikačních prací Theses.cz provozovanou Národním registrem vysokoškolských kvalifikačních prací a systémem na odhalování plagiátů.

České Budějovice, April 25, 2014

….....
Bc. Zuzana Kotrbová

Acknowledgments

Na tomto místě bych ráda nejprve poděkovala své školitelce Aleně Zíkové za příležitost pracovat v její laboratoři. Také bych jí chtěla poděkovat za její vedení, naučení základní technik a ochotu pomoci vždy, když jsem to potřebovala. Dále bych chtěla poděkovat Káje a Míše, které mi ukázaly základní metody a vždy se mi snažily odpovědět na mé dotazy. Ráda bych také poděkovala paní doktorce Daně Hockové z Ústavu Organické chemie a Biochemie za poskytnutí inhibitorů použité v této práci.

Mé díky patří také celému ostatnímu kolektivu: Brianovi, Davidovi, Ondrovi, Evě, Hance, Honzovi a Ance, kteří mi pomohli, kdykoliv jsem potřebovala a zároveň vytvořili příjemné pracovního prostředí.

Dále bych chtěla poděkovat celé své rodině za porozumění a morální i finanční podporu. Děkuji mamce, která mě zásobila kosmetikou, vitamíny, dobrý jídlem a moudrými radami, že jsem to díky ní zvládla. Děkuji taťkovi za to, že se i přes své starosti zajímal o mojí práci. Děkuji Gábince za pomoc na dálku, i když měla svých problému více než dost. Na závěr bych chtěla poděkovat svým morčátkům, Cecilkovi (†16.4. 2014) a Kryšpínkovi za to, že jsem se v těžkých chvílích měla s kým pomazlit, a za to že pohled na ně mi vždy dodal sílu.

Content

1 Introduction

1.1 *Trypanosoma brucei*

Trypanosoma brucei is a parasitic protist belonging to the order Kinetoplastida that also includes another unicellular parasites such as *Trypanosoma cruzi* and *Leishmania spp.*. There are three subspecies of *T. brucei*: *T. b. brucei*, *T. b. gambiense* and *T. b. rhodesience*. *T. b. gambiense* and *T. b. rhodesience* are etiological agent of the African sleeping sickness in 36 countries in West and Central Africa. *T. b. gambiense* is responsible for 98% cases of this very serious illness. Nearly 50 millions of people are living at the risk of acquiring the disease. A half million of people are infected and ~20 000 patients die annually. *T. b brucei* infects cattle and also wild animal causing a disease named nagana which brings enormous disease burden to regions where grazing cattle are major source of milk and meat. (http://www.who.int/en/).

T. brucei has a complex life cycle including two very different hosts, mammals and a tsetse fly (*Glossina spp.*). Due to this fact, *T. brucei* must undergo large structural and metabolic changes in cell morphology and metabolism. In the tsetse fly, *T. brucei* dwells in the gastrointestinal track as a procyclic stage. From the gastrointestinal tract, it moves to the salivary glands, where it develops as a metacyclic form capable of being to be transfer to the new host (Volf *et al*., 2007; Matthews *et al*., 2004). In the new host, a mammal, *T. brucei* occurs in the blood and other tissue fluids as a bloodstream form. To evade immune attack, *T. brucei* developed a variant surface glycoprotein (VSG) coat that is changing during the infection. Therefore, VSG coat confounds the immunity system and *T. brucei* is protected (McCulloch, 2004; Pays *et al.*, 2004). During the course of infection, the bloodstream form develops to the non-proliferative stumpy form. Subsequently, the stumpy form is sucked by a tsetse fly and the life cycle is complete (Matthews *et al*., 2004; Figure 1.1). In mammals, there are two stages of the infection. During the first stage, *T. brucei* is multiplying in the blood and lymph, and this stage is accompanied by symptoms like fever, headaches, joint pains and itching. During the second stage the parasite penetrates through the blood-brain barrier and infects the central nervous system. Typical symptoms for this stage of sleeping sickness are behavioral changes, confusion, sensory disturbances, poor coordination and disturbed sleep cycle. Ultimately, the sleeping sickness is always fatal without a proper treatment (http://www.who.int/en/).

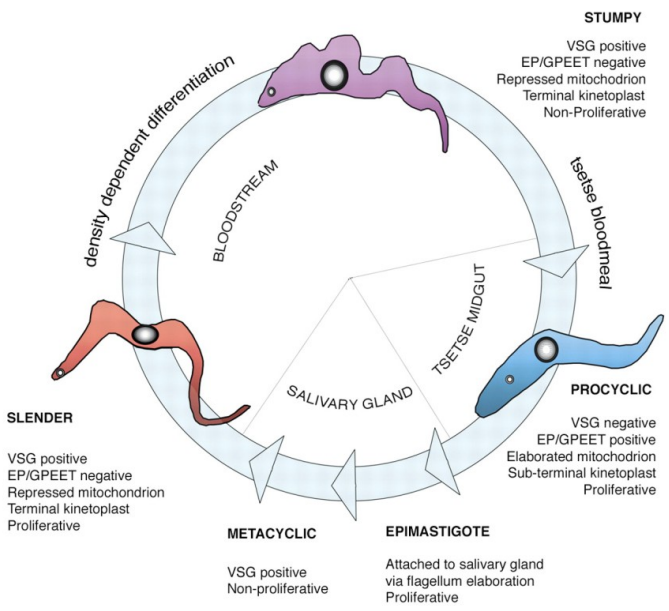

Figure 1.1: Life cycle of *T. brucei*.

Trypanosomes proliferate in the mammal's bloodstream as a bloodstream form. With increasing number of parasitic cells, a stumpy cells appear. This stage does not multiple and it is ready for a transmission to tsetse fly. After the bloodmeal, *T. brucei* cells start proliferating in the gastrointestinal track of tsetse fly as a procyclic form. After settling, *T. brucei* is arrested in growth, and it moves to the salivary glands, where it reaches a stage of epimastigote. These proliferating cells transform to a non-proliferating metacyclic form which is ready for transmission to the new mammal host (Matthews, 2005).

Sadly, the available drugs suffer from being inefficient, obsolete and difficult to administrate. Moreover, they possess toxic effects for patients because of some of them being mutagenic and carcinogenic (Croft *et al*., 2005). Therefore, it is necessary to find appropriate drugs to treat diseases caused by *Trypanosoma* parasites. Several main points must be followed for the production of new anti-parasitic drugs. The drug must be stable, orally administered and effective against the parasite while being harmless to the human host. The production of the new chemotherapeutic must be at low cost. Moreover, the bioavailability and the possibility of resistance development must be considered when new drugs are released (de Jersey *et al.*, 2011).

Because purine acquisition in *Trypanosoma* and *Leishmania* cells is an indispensable nutritional process, and because parasites do not possess *de novo* pathway to produce purines, the enzymes of the purine salvage pathway are considered as attractive targets for therapeutic development (Berg et al., 2010b).

1.2 Purine Salvage Pathway

The purine and its nucleobases (Figure 1.2) are essential molecules for life. Purine nucleotides serve as a nucleic acid precursor, a modulator of enzyme activity, a component

of coenzymes like ATP, GTP, NADH, the acetyl coenzyme A, and they are precursors for the synthesis of the second messenger cyclic AMP (Berg *et al.*, 2010b).

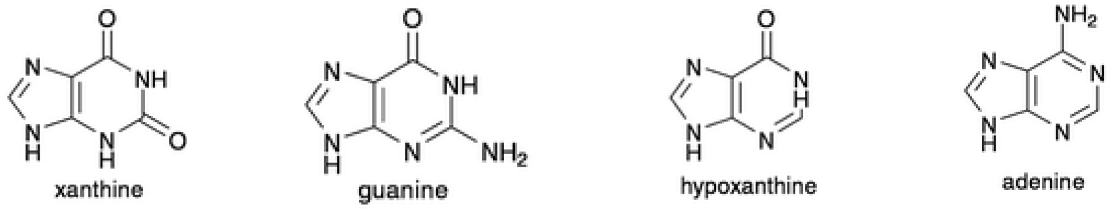

Fig. 1.2. Most common purine nucleobases.

Purine nucleobases can be synthesized in cells by two different ways: by the *de novo* biosynthesis or by the purine salvage pathway (PSP). Using the *de novo* biosynthesis, inositol monophosphate (IMP), that can be transfer to other nucleobases or nucleotides like GMP or AMP, is created from simple precursors like glycine (Berg *et al.*, 2010b). On the other hand, PSP exploits the exogenous purine sources followed by in-cell metabolism of these molecules (Lawton, 2005). Unlike mammals, *T. brucei* and nearly all parasitic protozoa are auxotrophic for purines and they cannot synthesize purine by *de novo* biosynthesis (Berriman *et al*., 2005). Given that, this pathway is the only way for *T. brucei* how to obtain essential purine molecules, and the purine salvage pathway is considered to be a potential drug target.

Various parasites have different preferences for purine nucleobases. For example, *T. brucei* and *T. cruzi*, intracellular parasite from South America causing Changase disease, uptake adenine as the most favorable purine, followed by hypoxanthine and guanine. Xanthine is the least preferred source of purine. Nucleosides are uptaken in a similar order (Berg *et al.*, 2010a). Hypoxanthine and adenine are the major sources of purine in the blood, though adenine appears in considerably less concentrations (Vodnala *et al*., 2008).

In a case of extracellular parasite like *T. brucei*, the host purines must cross only the cell plasma membrane while in a case of intracellular parasites, like *T. cruzi*, *Leishmania* and *Plasmodium*, the purines must go through host's plasma membrane, across the parasitophorous vacuole membrane and the parasite's cell membrane (Berg *et al.,* 2010b). Although a simple diffusion seems to be plausible to obtain essential purines, an efficient purine uptake is enabled by nucleoside/nucleobase transporters (de Koning and Jarvis, 1997). In the genome of *T. brucei*, 12 nucleoside transporters have been identified, and it is still unclear why *T. brucei* needs so many of them. There are two nucleoside transporters, P1 and P2, and four nucleobase transporters, H1, H2, H3, H4 (Berg *et al.,*

2010b). P1 nucleoside transporter allows adenosine, inosine, guanosine and sometimes hypoxanthine to cross the plasma membrane, and this receptor is expressed in both life stages of *T. brucei* (Ortiz *et al*., 2009; Sanchez *et al*., 2002). P2 nucleoside transporter enables transport of adenosine and adenine, and only a bloodstream form expresses this transporter (Mäser *et al*., 1999). The nucleobases transporters H1-H4 facilitate import of all types of nucleobases, though H1 and H4 transporters are expressed only in the procyclic form and H2 and H3 are found in the bloodstream form (de Koning *et al*., 2005).

Once the host's purines are inside of the parasitic cell, the enzymes of purine salvage pathway are responsible for their modifications, conversion and metabolism (Figure 1.3).

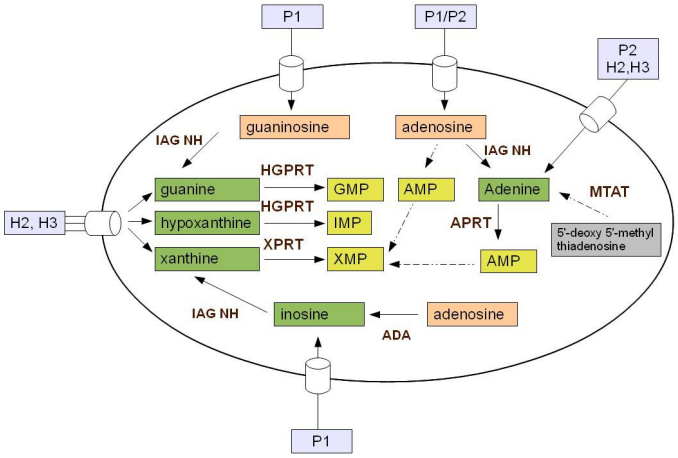

Figure 1.3: Purine salvage pathway in *T. brucei*.

Inosine-adenosine-guanosine nucleoside hydrolase (IAG-NH), inosine-guanosine nucleoside hydrolase (IG-NH), methylthioadenine phosphorylase (MTAP), adenine phosphoribosyl-transferase (APRT), hypoxanthine-guanine phosphoribosyltransferase (HGPRT) adenosine deaminase (ADA) and adenosine kinase (AK) (Berg *et al.*, 2010b).

Nucleoside hydrolases (NH), methylthioadenine phosphorylase (MTAP) and phosphoribosyltransferases (PRT) belong to N-ribosyl transferases. These transferases catalyze reactions that transfer a purine from or to ribose or deoxyribose. NH and MTAP split the nucleoside bond between the sugar residue ribosyl and aglycon using water or phosphate molecule. Two types of NH were discovered in cell of *T. brucei*: Inosine-adenosine-guanosine nucleoside hydrolase (IAG-NH) and inosine-guanosine nucleoside hydrolase (IG-NH) (Parkin, 1996; Pellé *et al*.,1998; Verseés *et al*., 2001). IG-NH is known as 6-oxopurine specific and it has a greater affinity to guanosine and inosine while IAG-NH is purine nucleoside specific with high affinity especially for adenosine (Vandemeulebroucke *et al.*, 2010). Since NH activity has not been detected in the mammalian cell, these enzymes can be potential drug targets against trypanosomas (Berg *et al.*, 2010a). In contrast to cleaving activities of NH and MTAP, PRTases are binding enzymes and transfer phosphoribosyl to free nucleobase such as adenine, xanthine, hypoxanthine and guanine.

Depending on the type of nucleobase, three types of PRTases are distinguished in the cell of *T. brucei*: hypoxanthine-guanine phosphoribosyltransferase (HGPRT), xanthine phosphoribosyltransferase (XPRT) and adenine phosphoribosyltransferase (APRT). PRTases are present in both parasitic protozoa cells and mammalian cells (Berg *et al.*, 2010a).

As it has been mentioned before, the purine salvage pathway in *T. brucei* is a potential drug target. Inhibitors targeting IAG-NH, MTAP and adenosine kinase (AK) are of the main biological interest, however the inhibition of these enzymes can be bypassed by an uptake of simple purine bases (Berg *et al.*, 2010b). Since nucleobases as adenine, hypoxanthine, xanthine and guanine may be converted to the appropriate nucleoside using enzymatic activity HGPRT, XPRT and APRT, parasites can survive on simple purine sources like hypoxanthine and adenine (Pellé *et al*., 1998; Reyes *et al*., 1982;Verseés *et al*., 2001,). Thus, the purine salvage pathway seems to be versatile and the inhibition of one enzyme is inefficient. Therefore, the treatment must be complex and it must include at least two different inhibitors (Berg *et al.*, 2010b).

1.3 6-oxopurine phosphoribosyltransferases

6-oxopurine phosphoribosyltransferases (6-oxopurine PRTases) belong to the bigger family of ten different enzymes that synthesize purine nucleotides, pyrimidine nucleotides and NAD. 6-oxopurine PRTases catalyze reaction between phosphoribosyl and 6-oxopurine nucleobase (Figure 1.4).

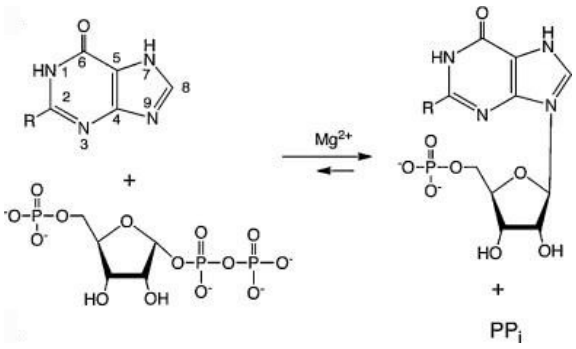

Figure 1.4: Reaction catalyzed using 6-oxopurine PRTases. Nature occurring bases are guanine (R is -NH2), hypoxanthine (R is -H) a xanthine (R is -OH) (Kehoug *et al*., 2009).

For this catalytic reaction, a divalent metal ion must be present, and in many cases this ion is magnesium Mg^{2+} (de Jersey *et al.*, 2011). Exact enzymatic mechanism of 6-oxopurine PRTases is known only for the human 6-oxopurine PRT, since its crystal structure has been

solved (Eads *et al*, 1994; Figure 1.5). However other PRTases will most likely follow the same reaction mechanism. The reaction starts when divalent metal ion binds to phosphoribosyl, then the purine base comes to the reaction center followed by pyrophospate dissociation and the formation of nucleoside monophosphate is (de Jersey *et al.*, 2011).

Interestingly, in addition to the divalent metal ion, a large flexible loop is another common feature for 6-oxopurine PRTases (Figure 1.5). This loop is comprised of ten to twenty amino acids and it plays a role in closing around the enzyme active site during the catalytic reaction. Thus, the transmission of nucleoside is stabilized and the bond between ribose and pyrophospate can be formed (Krahn *et al.*, 1997).

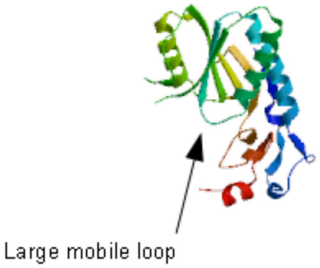

Figure 1.5: Subunit A of human HGPRT (Swiss-model template library)

Various 6-oxopurine PRTases from different organisms can be divided according to their specificity to individual natural occurring purine bases (guanine, hypoxanthine and xanthine) and regarding their affinity (K_{cat}) values to their appropriate substrates. For example bacterial PRTases are the most efficient enzymes being 4-7 times more effective in comparison to human PRTase. Some of the PRTases can use as substrate all of three nucleobases, some of them has affinity to two different ones and some enzymes are highly specific to only one special nucleobase. Many organisms including human have only one 6-oxopurine PRTase (de Jersey *et al.*, 2011).

6-oxopurine PRTases are important in all living organism, and due to this fact, they have a common structure and catalytic features. However, in different organisms 6-oxopurine PRTases convert distinct substrates, and they possess differences in their catalytic activities. For example, mammalian PRTases have no affinity to xanthine while this nucleobase is a preferential substrate for the trypanosomas' XPRT (Berg *et al.*, 2010a). Thus, it is possible that inhibitors of 6-oxopurine PRTases will selectively inhibit parasite's enzyme and cause a death of this infectious agent. Furthermore, it has been shown that people with mere 3% activity of HGPRT live without major problems (Dawson *et al*., 2005). Therefore, a partial inhibition of human HGPRT using anti-parasite inhibitor should not affect the patient's life. Taking this information together, it is reasonable to investigate the function

and activity of parasitic PRTases to evaluate these enzymes as potential drug targets and to inhibitors of PRTases for their selective inhibitory properties.

6-oxopurine PRTases were extensively studied in cells of *Leishmania donovani*, a parasitic protozoa causing a visceral leishmaniasis (Volf *et al*., 2007). *L. donovani* possesses the same enzymes as *T. brucei*: HGPRT, XPRT and APRT (Hwang and Ullman, 1997). Furthermore, it was reported that HGPRT and XPRT enzymes are essential for parasite viability, infectivity and purine acquisition (Boitz and Ullman, 2006a). In additional, HGPRT and XPRT were surprisingly localized to the glycosome (Shih *et al.,*1998), the specialized subcellular organelle unique for Kinetoplastida (Michels et al., 2006). Glycosomes are peroxisome-like organelles (Gauldron-Lopéz and Michels, 2013), and they contain many metabolic pathways which normally occurred in the cytosol like glycolysis, ether lipid biosynthesis, sterol and isoprenoid biosynthesis, gluconeogenesis, pyrimidine biosynthesis, β-oxidation, pentose phosphate pathway and purine salvage pathway. Many of these enzymes and pathways are essential for *T. brucei* (Colasante *et al.,* 2006), and a mislocation of these important proteins to the cytosol leads to the cell death (Brennand *et al.,* 2012). Peroxisomal and glycosomal proteins are synthesized using cytosolic free ribosomes (Brennand *et al.,* 2012; Gauldron-Lopéz and Michels, 2013), and their localization is determined by the glycosomal or the peroxisomal-targeting signal (PTS). PTS can be located at the C-terminal end of the protein (PTS1), or it can be found at the N-terminus (PTS2). PTS1 consists of three amino acid of SKL motif where first amino acid is small uncharged, second one contains a hydrogen binding group, and the last one is of the hydrophobic nature. PTS2 is defined by a more complex nonpetide motif (Gauldron-Lopéz and Michels, 2013). Moreover, there is a variable internal PTS, called I-PTS (Penha, *et al.,* 2009). Both HGPRT and XPRT from *L. donovani* contain well defined PTS1 targeting signal (Boitz and Ullman, 2006a).

Likewise in *L. donovani*, 6-oxopurine PRTases were extensively studied in one of the most serious human parasitic pathogen, *Plasmodium*, an infectious agent of malaria. (Schmidt and Roberts, 2009). *P. falciparum* possesses three key purine salvage enzymes: adenosine deaminase (ADA), purine nucleoside phosphorylase (PNP) and hypoxanthine-guanine-xanthine phosphoribosyltransferase (HGXPRT) (Zhao *et a.l*, 2012). PNP has similar function as already mentioned NH in *T. brucei*. Interestingly, PNP and NH enzymes have never been found together in one organism (de Jersey *et al*., 2011). Unlike *T. brucei* or *L. donovani*, *P. falciparum* has only one 6-oxopurine PRT (HGXPRT), whose main substrate

is hypoxanthine (Abdelwahab *et al.,* 2012). Recently, analogs of mononucleotides were designed and explored as potential inhibitors of this 6-oxopurine PRT. These inhibitors are called acyclic nucleoside phosphonates (ANPs). Importantly, the ANPs inhibit the HGXPRT enzyme *in vitro* and they hinder the growth of *Plasmodium* cells *in vivo* (Keough *et al.*, 2009; De Clercq, 2013).

1.4 Acyclic nucleoside phosphonates

Acyclic nucleoside phosphonates (ANPs) are 2-(phosphonoalkoxy)alkyl derivatives of purine and pyrimidine bases. ANPs consist of purine base and phosphate group mimicking the 5'– phosphate group link to the ribose (De Clercq, 2012). There are three main differences between ANPs and mononucleotides (Figure 1.6). First, there is a replacement of oxygen ester with carbon. This replacement provides resistance to the enzymatic dephosphorylation or chemical hydrolysis. Second, there is a displacement of oxygen atom. The classic atomic arrangement of nucleotides is C-O-P, but the arrangement of ANPs is O-C-P. This difference causes greater resistance to the degradation of ANPs compared to the normal nucleotide. The last difference is an absence of the glycosidic bond that further increases the resistance to the degradation. Moreover, ANPs are very flexible in their structure. This flexible structure enables conformational changes important for the binding to the active site of the enzyme (Keough *et al*., 2009).

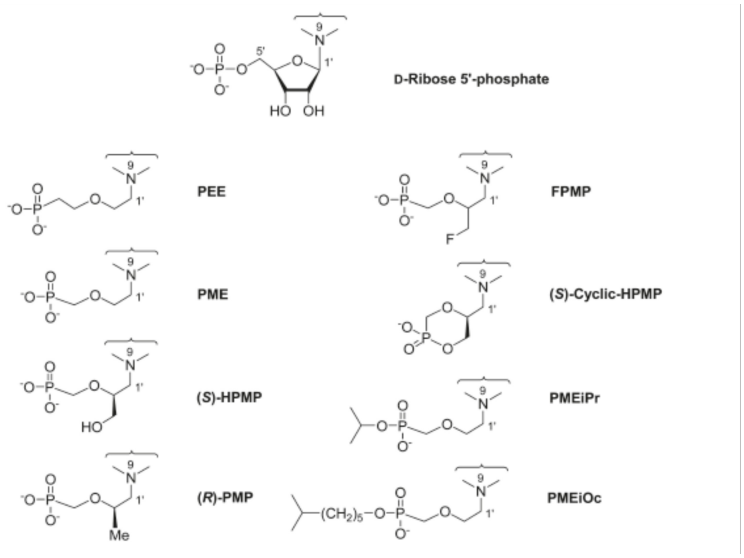

Figure 1.6: Differences between mononucleotides and some ANPs (Keough *et al*., 2009)**.**

Chemical and pharmaceutical properties of ANPs are objects of intensive studies due to their antiviral and antiparasitic activity (Holý, 2005) and their non-toxicity for human cells (Česnek *et al*., 2012). Currently, quite a few ANPs are in clinical use to treat serious viral

diseases (Figure 1.7). The most famous ANPs are (S)-9-(2,3-Dihydroxypropyl)adenine [(S) DHPA, known commercially as Duviragel], (S)-1-(3-Hydroxy-2-phosphonomethoxy-propyl) cytosine [(S)-HPMPC, known as Cidovir or Vistide,] or 9-(2-Phosphono-methoxyethyl) adenie (PMEA, Adefovir). Duviragel is an aliphatic nucleoside analog with broad-spectrum of antiviral activity, and it is used to treat infection by herpes labialis. Cidovir has been used to treat cytomegalovirus retinitis in AIDS patients and in other immunosuppressed patients since 1996. Moreover, Cidovir can be used against human papillomavirus infection, polymavirus infection and even smallpox. Adefovir was originally developed as a potent drug against HIV virus. However, the dose required to eliminate HIV infection was too high and thus toxic for the patients, yet this drug is used to cure hepatitis B virus infection. Finally more effective Tenofir [(R)-9-(2-Phosphonomethoxypropyl)adenine, (R)-PMPA] was introduced to the market to treat HIV infection (De Clercq, 2013).

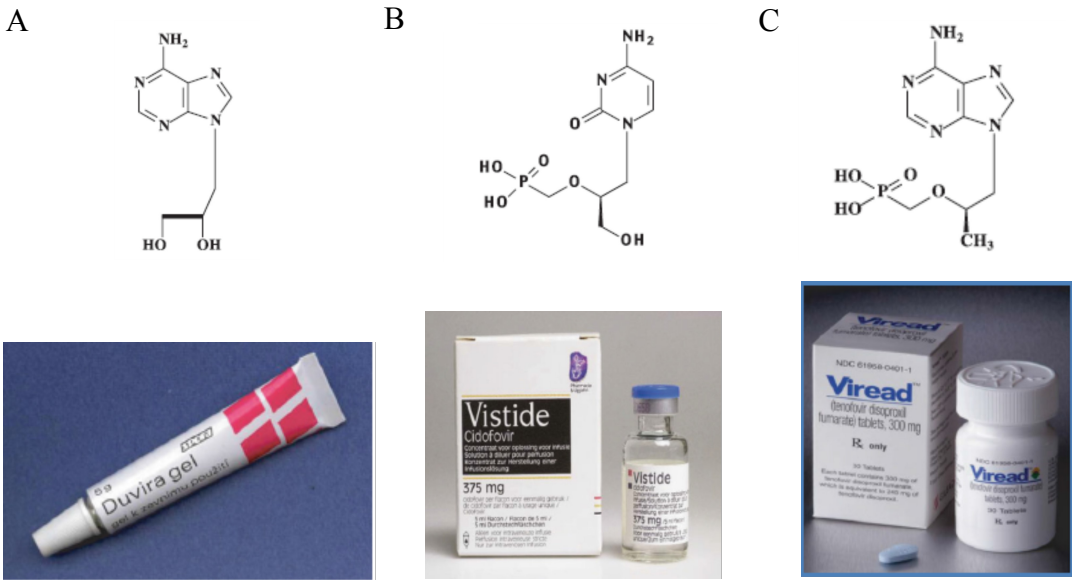

Figure 1.7: Examples of ANPs in current clinical use.

A: (S)-DHPA, Duviragel

B: (S)-HPMPC, Vistide

C: (R)-PMPA, Tenofir and its fumarate salt known as Viread

(De Clercq, 2013)

As it was mentioned above, ANPs also possess antiparasitic activity, and they were at first tested on *Plasmodium* cells. ANPs, which inhibit *Plasmodium* HGXPRT, include (S)-HPMPG (similar to Vistide, but containing guanine instead of cytosine) and PMEG (similar to Adefovir, containing guanine instead of adenine) (De Jersey *et al*., 2011). First evidence of inhibition HGXPRT by ANPs was observed in 1999 (Smeijsters *et al*., 1999),

but the mechanism of their action was unclear until the crystal structures of PfHGXPRT bound with PPi.Mg^{2+} and human HGXPRT inhibited with acyclic guanosine phosphonate were solved (De Jersey *et al*., 2011).

There are three key enzyme regions that are responsible for the inhibitor binding: the 5'-phosphonate binding site, the large mobile loop and the purine binding site. The 5'-phosphonate binding site is a loop that changes radically its structure when a mononucleotide product or a transition state analogue or a phosphonate binds to the active site. The phosphonate group's oxygen then creates tight hydrogen bonds with this loop due to close interaction between the enzyme and ANP. The second important region is the large mobile loop that needs the Mg^{2}+ ion and phosphoribosyl to change its structure and to close up the active side. The last key region, the purine binding site, provides the selectivity and the affinity. When nucleobase as hypoxanthine or xanthine is linked to either ribose-5'-phosphonate or ANP and binds to the active site, it triggers the displacement of the hydrogen bond inside of the purine binding side and forming of new hydrogen bond between the purine binding side and the oxygen atom of the purine ring (Keough *et al*., 2009). Additionally, the length of ANP is also important. Binding of short ANP is annulled. On the other hand, longer ANP does not bind also, because ANP is too long to bridge the purine binding site and the 5'-phosphate binding site. (Keough *et al*., 2009)

Since *T. brucei* posseses two 6-oxopurine PRTases (HGPRT and XPRT), we decided to test if selected ANPs will inhibit these enzymes. Furthermore, it has been reported in the past that some types of ANPs [e.g. (S)-HPMPA] have cytotoxic effects on *T. b. rhodosience*, *T. b. gambience* and *T. b brucei* cells (Kaminsky *et al*., 1998;Kaminsky *et al*., 1996). Additionally, it seems that some ANPs can cross blood-brain barrier, so they can be used to treat second stage of the infection (Freeman and Gardiner,1996).

ANPs are synthesized in the former lab of Prof. Holy, which is now led by Dr Zlatko Janeba (Institute of Organic Chemistry and Biochemistry, Prague CZ). Over 100 different derivatives of ANPs were provided to us by Dr. Dana Hockova from the same lab. Having an opportunity to work with such a wonderful library, we have initiate studies to characterize *T. brucei* HGPRT/XPRT proteins and to decipher mode of action of selected ANPs.

2 Aims

1. Assess biological roles of TbHGPRT/1, TbHGPRT/2 and TbXPRT enzymes *in vivo*
2. Over-express and purified recombinant TbHGPRT/1 and TbXPRT proteins
3. Establish *in vitro* activity assays of purified TbHGPRT/1 recombinant protein
4. Determine the IC_{50} values for selected ANPs *in vivo*

3 Materials and Methods

3.1 Cloning

3.1.1 Primer design and Polymerase Chain reaction (PCR)

There is a single gene (Tb927.10.1390) encoding XPRT while there are two genes encoding HGPRT proteins (Tb927.10.1400, HGPRT/1; Tb927.10.1470, HGPRT/2). Nevertheless, HGPRT/1 and HGPRT/2 are very similar at the nucleotide and amino acid level (Figure 4.1) with only several amino acids being different at the C-terminus.

For the purpose of this study, HGPRT/1, HGPRT/2 and XPRT genes were cloned to different vectors: pBSK3 (Chen *et al.*, 2004), pT7v5 (Flaspohler *et al*., 2010) and p2T7-177 (Wickstead *et al.*, 2002). pBSK3 vector is used to over-express proteins tagged with His tag in the bacterial cells. pT7V5 vector is used to over-express proteins tagged with v5 in *T. brucei* cells. p2T7-177 plasmid is used to produce dsRNA and thus silence an expression of the protein of interest in *T. brucei* cells. First, the genes were amplified by PCR using primers containing different restriction sites (see Table 3.1).

Table 3.1: Primers for PCR amplification. Underlined sequence are specific restriction sites.

Expresion in pSKB3	**Primer sequence**	**Restriction site**
TbXPRT Fw	CAC<u>GGATCC</u>CACTCGGGCCATCCTCTC	BamHI
TbXPRT Rv	GTG<u>CTCGAG</u>TTACAATTTGCTCGGGTACC	XhoI
TbHGPRT/1 Fw	CAC<u>GGATCC</u>GAACCAGCTTGCAAATACG	BamHI
TbHGPRT/1 Rv	GTG<u>CTCGAG</u>TTACCGCTTGGCTTCTCC	XhoI
Over-expression in pTv5		
TbXPRT Fw	CAC<u>GGATCC</u>CACTCGGGCCATC	BamHI
TbXPRT Rv	CAC<u>TCTAGA</u>TTACAATTTGCTCG	XbaI
TbHGPRT/1 Fw	TAC<u>GGATCC</u>GAACCAGCTTGCAAATAC	BamHI
TbHGPRT/1 Rv	GCG<u>TCTAGA</u>TTACAGTTTTGCCTTCACAGC	XbaI
TbHGPRT/2 Fw	CAC<u>GGATCC</u>GAACCAGCTTGCAAATAC	BamHI
TbHGPRT/2 Rv	GCG<u>TCTAGA</u>TTACAGTTTTGCCTTCACAGC	XbaI
RNAi in p2T7_177		
TbXPRT Fw	CAC<u>AAGCTT</u>TGCACTCGGGCCATCCTCTCA	HindIII
TbXPRT Rv	CAC<u>CTCGAG</u>GTACGCCCCGTGTCGGCAAT	XhoI
TbHGPRT Fw	GAC<u>GGATCC</u>ACGACTTCGCAA	BamHI
TbHGPRT Rv	GTG<u>AAGCTT</u>GTCGATAGCCACG	HindIII

The PCR was carried at Thermal Cycler (Biorad) under following conditions:

1. Denaturation 96ºC 5 minutes
2. Denaturation 94ºC 0.5 minute
3. Primer annealing 55ºC 0.5 minute
4. Amplification 72ºC 1 minute
5. Amplification 72ºC 10 minutes
6. Hold at 4ºC

Steps 2, 3 and 4 were repeated 30-times.

PCR products were visualized on the agarose gel, the proper size was checked using a known DNA ladder, and the amplified DNA was extracted from the gel using QIAquick Gel Extraction (QIAGEN).

3.1.2 pGEM-T easy cloning and *E. coli* transformation

The purified PCR products were ligated to the pGEM®-T easy Vector System (Promega) (Figure 3.1) accordingly the manufacturer's instruction.

After the ligation step, the reaction was transformed to *E. coli* strain XL1 (5µl of ligation reaction into 50µl of the bacterial culture). Cells were incubated on ice for 10-20 minutes followed by a heat shock (45 seconds at 42ºC). Then cells were cooled down on ice for 2 minutes, 250µl of SOC medium was added, and cells were incubating for 45-75 minutes at 37ºC in the shaking incubator. In a meantime, 50µl of 100mM IPTG and 30µl of X-gal (at 200mg/ml) were added to the agarose plate containing ampicillin

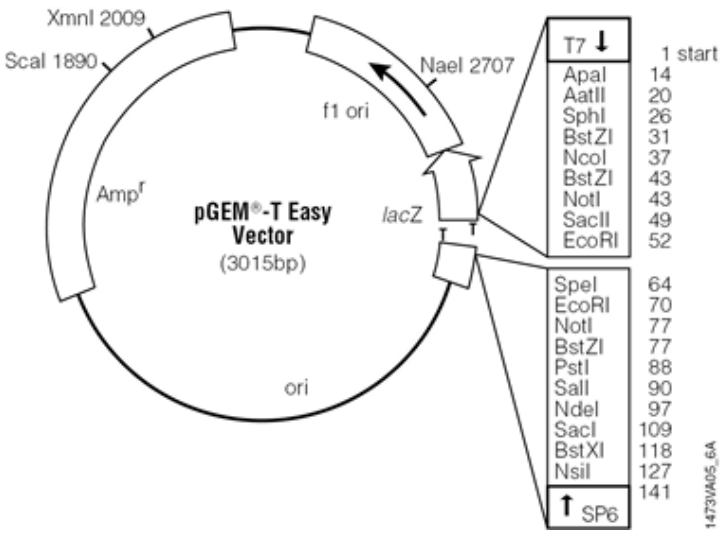

Figure 3.1: Map of commercial vector pGEM®-T easy (Promega).

(100µg/ml) to select cells contacting correct plasmid using blue/white selection screen. Cells were spread on the plate, incubated at 37ºC over night, and white colonies were picked up to following analyzes. Single colonies were grown in 5ml of LB media overnight at 37ºC in the shaking incubator. Plasmid DNA was isolated by QIAprep Spin Miniprep Kit (QIAGEN) using manufacturer's protocol, and plasmid DNA was verified using restriction reaction with the appropriate restriction enzymes and by sequencing. Restricted fragments carrying targeted genes were isolated from the agarose gel and used for subsequent cloning step to pBSK3, pTv5 N-terminus and p2T7-177 vectors.

3.1.3 Preparation of pTv5-N-terminal vector

In order to create a plasmid that would contain the v5 tag at its N-terminus (pTv5-N-term), the original pTv5 plasmid (containing v5 tag at its C-terminus; Figure 3.2 A) was mutated using QuikChange Lightning Multi Site-Directed Mutagenesis Kit to create XbaI restriction site before the 3xv5tag sequence. In the second step, the 3xv5 tag were amplified by PCR and pGEM®-T easy. The 3xv5tag was cloned between T7 promoter and place for gene of interest using HindIII and BamHI restriction enzymes. Finally, the original 3xv5tag was cut out with BamHI and XbaI restriction enzymes (Figure 3.2 B). This modified vector was used to over-express XPRT and HGPRT genes in *T. brucei.*

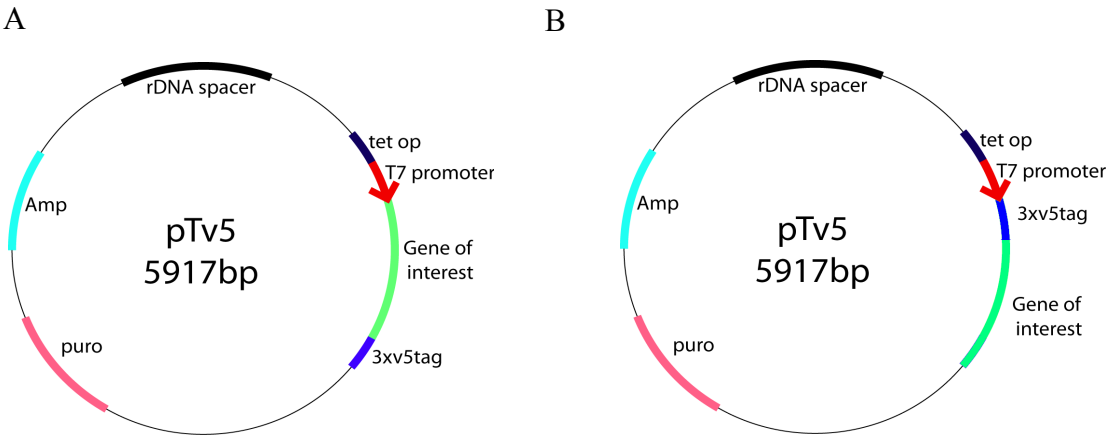

Figure 3.2: Map of original pTv5 vector (A) and modification to create pTv5-N terminal (B).

3.1.4 Ligation to pSKB3 vector, pTv5-N-terminal vector and p2T7_177 vector

Maps of pSKB3 vector and p2T7_177 are on Figure 3.3.

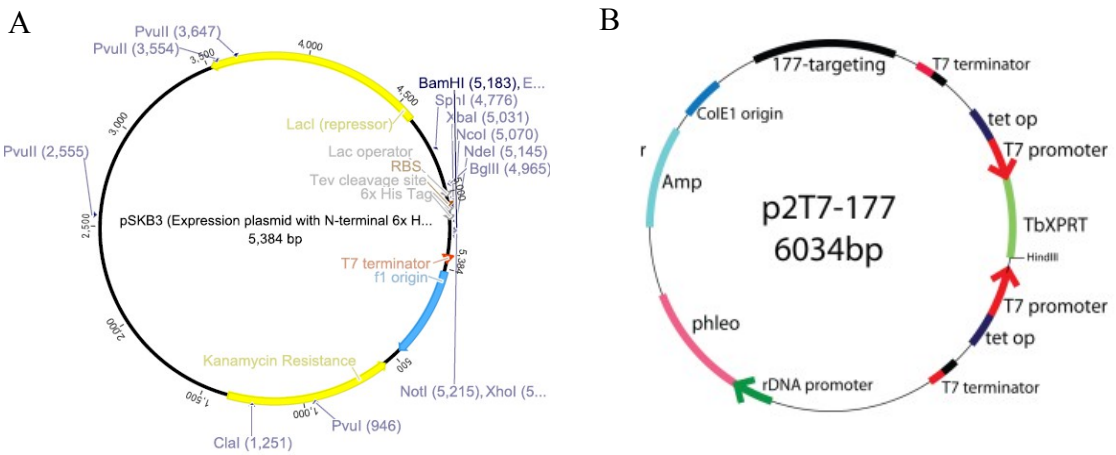

Figure 3.3: Maps of pSKB3 vector (A) and p2T7_177 vector (B).

Vectors were cleaved with particular restriction enzymes (Table 3.2). Restrictions were proved on the agarose gel, and restricted vectors were isolated from the gel followed by ligation of the specific inserts. In case of p2T7_177, fragment of TbHGPRT was cloned at first followed by cloning of TbXPRT fragment. Success of ligation was verified using specific restriction enzymes and by sequencing. Verified vectors pSKB3 carrying specific inserts were transformed to *E. coli* strain BL21, and proved vectors pTv5-N-term and p2T7_177 were electroporated to *T. brucei* cells.

Table 3.2: Vectors and their inserts.

Vector	Purpose	Restriction enzymes	Genes
pSKB3	Over-expression in *E. coli*	BamhI, XhoI	TbXPRT, TbHGPRT/1
pTv5-N-Term	Over-expression in *T. brucei*	BamHI, XbaI	TbXPRT, TbHGPRT/1, TbHGPRT/2
p2T7_177	RNAi in *T. brucei*	BamHI, HindII, XhoI	Fragments of TbXPRT and TbHGPRT

3.1.5 Electroporation, antibiotic selection and cultivation of *T. brucei* bloodstream form cells

Verified plasmids p2T7-177/TbHGPRT+TbXPRT, pTv5-N-term_TbXPRT, pTv5-N-term_TbHGPRT/1 and pTv5-N-term_TbHGPRT/2 (20ug) were cleaved by NotI restriction enzyme (1.5ul) at 37ºC overnight. The Not1 enzyme cleaves specific sequence that is homologue to the rDNA in the case of pTv5 plasmid or transcriptionally silent 177 region in the case of p2T7-177 plasmid of *T. brucei*, and thus directs this plasmid to

the genome by homologue recombination. Linearized constructs (50ul reaction) were precipitated by 5µl of 3M sodium acetate and 125µl 96% ethanol, air-dried and resuspended in the sterile water.

A specific single marker (SM) cell line was used to introduce linearized plasmid DNA into the genome. SM cell line is genetically modified cell line of *T. brucei* BF427 containing the T7 polymerase and the tetracycline repressor under the G418 selection. These two genes products enable inducible expression of the gene of interest in pTv5-N-term or expression of dsRNA in p2T7-177. SM are kept under the G418 selection at the concentration of 2.5µg/ml in HMI-9 medium (HMI-9/G).

To transfect cells with the linearized plasmid, approximately $3x10^7$ SM cells were harvested by centrifugation. The cell pellet was washed with 20ml of sterile PBS-G and resuspended in 100µl AMAXA human T-cell solution. Cells were placed into the electroporation cuvette and 10-15µg of precipitated linearized plasmid DNA was added. Electroporation was conducted using the Nucleofector II (Amaxa) X-001 program, after which the transfected cells were transferred to 30ml HMI-9/G. 10-fold serial dilutions of the transfected cells ($1x10^7$, $1x10^6$ and $1x10^5$) were dispensed into 24-well plates and left to recover for 16h at 37ºC in 5% CO2. Then 1ml of HMI-9 with phleomycine (final concentration 2.5µg/ml, HMI-9/G/Phleo;) was added into every well for p2T7-177 vector (p2T7-177 bears resistance for phleomycine), and 1ml of HMI-9/G with puromycine (final concentration 0.1µg/ml, HMI-9/G/Puro) was added for pTv5-N-terminal vector (pTv5 bears resistance for puromycine). Plates were incubated at 37ºC for up to 10 days until the antibiotics selection was completed and clones selected. Cells resistant to antibiotics underwent successful homologue recombination event. Through the study the bloodstream form *T. brucei* was kept in HMI-9 media (Hirumi *et al.*, 1997) with specific antibiotics at 37ºC under 5% CO_2 at the density of $1x10^5$ – $2x10^6$ cells/ml.

3.2 Expression and purification of recombinant protein TbHGPRT/1_6His and TbXPRT_6His

3.2.1 Pilot expression

To determined over-expression of TbHGPRT/1_6His and TbXPRT_6His, *E. coli* cells were growing in 5 ml LB media containing kanamycin (pSKB3 bears resistance for kanamycin) at 37ºC in the shaking incubator. When the OD_{600} reached 0.4, cells were induced with IPTG (final concentration 100µM). Right before the induction, 1ml of culture

was taken and harvested by centrifugation as a non-induced whole cell lysate (WCL) sample. Induced cells were left growing for one, two and three hour, and every hour 1ml of culture was harvested as an induced WCL sample. Expression was verified on the 12% SDS-PAGE gel and coomassie staining.

3.2.2 Solubility pilot assay

To assess a solubility of TbHGPRT/1_6His and TbXPRT_6His, the solubility pilot assay using Bug Buster solution (Novagen) was performed. Briefly, the cell pellet was prepared from 5ml of bacterial culture that was induced at OD600=0.4, for hours at 37°C. Right before the induction, 1ml of culture was taken and harvested by centrifugation as a non-induced WCL sample. Induced cells were left growing for one hour, and then 1ml of culture was harvested as a WCL sample and the rest of the culture was harvested for the solubility analysis. WCL samples were obtained by resuspending cell pellets in 100µl PBS and 50µl 3xSDS-PAGE loading dye. To assess if protein of interest is soluble or not, the cell pellets were resuspended in 200µl of the Bug Buster solution containing 1x protease inhibitors (Roche) and were rotated for 30 minutes in RT. Then cell lysates were centrifuged at 16,000xg for 20 minutes at 4ºC and supernatants were transferred to new eppendorf tubes. Supernatant volumes were measured that pellets were resuspended in 1xPBS at the same volume as supernatant samples. All samples were then analyzed by SDS-PAGE followed by coomassie staining, or proteins were blotted onto the PVDF membrane, probed with anti-His primary antibody (1:2000; Invitrogen) followed by anti-mouse secondary antibody (1:2000; Biorad).

3.2.3 HPLC Purification of TbHGPRT/1_6His

Accordingly to the result of the solubility pilot assay, soluble TbHGPRT/1_6His was purified under native conditions. The cell pellet was prepared from 500ml of bacterial culture that was induced at OD600=0.4 for 2 hours at 37°C. The cell pellet was resuspended in STE buffer with 2x protease inhibitors. The volume of buffer was adjusted to the weight of the cell pellet (30 ml STE/1g of pellet). Cells were lysed with 1% Triton X-100 and freshly prepared lysozyme (30mg/1g of pellet) on ice for 30 minutes followed by DNAse I treatment (150µg/1g of pellet and 30mM $MgCl_2$). The sample was rotated for 10 minutes at 4ºC and spun down at 10.000xg for 30 minutes at 4ºC. The supernatant was filtered with the 0.45µm filter to remove any particles before loading onto the Ni-NTA column (1ml Histrap™ HP, GE Healthcare) that specifically binds His-tagged proteins. TbHGPRT/1_6His

was purified using ÄKTA prime plus accordingly to the product manual. STE buffer was used as a buffer A, and STE containing 500mM imidazol was used as a buffer B. Flow through was collected in 5ml fractions. Then fraction size was change to 1ml and elution was performed using a linear gradient (50ml, 0.5ml/min from 0mM to 500mM imidazol). Flow through and elution fractions were collected and verified on the SDS-PAGE gel. Elution fractions containing recombinant TbHGPRT/1_6His were pooled together and dialyzed against STE buffer with no imidazol using a dializing tube with 3,5kDa pores (Serva). The dialyzed recombinant protein was checked by SDS-PAGE, and its concentration was measured using Bradford protein assay (BioRad) with BSA as standards. 2.7mg of recombinant protein TbHGPRT_6His was sent for the antibody production to Davids Biotechnology (Regensburg, Germany), and it was also used in *in vitro* assays.

3.2.4 HPLC Purification of TbXPRT_6His

Accordingly to the result of the solubility pilot assay with Bug Buster, the insoluble TbXPRT_6His was purified using a protocol that used sarkosyl to solubilizate inclusion bodies. The cell pellet and cell lysate were obtained as mentioned above for TbHGPRT/1_6His protein. In contrast to the protocol above, the pellet after the Triton X-100 lysis (not the supernatant) was washed once with PBS and resuspended in PBS (15ml/1g of the cell pellet) containing 1.5%.sarkosyl. The sample was rotated at 4ºC overnight and spun down at 10.000xg for 30 minutes at 4ºC. The supernatant was filtered with the 0.45µm filter to remove any particles before loading onto the Ni-NTA column, and recombinant TbXPRT_6His was purified using ÄKTA prime plus accordingly to product manual under the same condition as for the purification of TbHGPRT/1_6His. Buffer A, and buffer B were (see chapter Solutions and Buffers) used during purification. Flow through and elution fractions were collected and verified on the SDS-PAGE gel. Elution fractions containing recombinant TbXPRT_6His were pooled together and were step dialyzed in two different buffers to decreases amounts of salts and to get rid off imidazole. The dialyzed recombinant protein was checked on the SDS-PAGE gel and its concentration was assessed by Bradford protein assay. The recombinant protein TbXPRT_6His was sent for an antibody production.

3.3 Measuring *in vitro* activity of TbHGPRT/1_6His

TbHGPRT/1_6His activity was measured by a continuous spectrophotometric assay measuring the conversion of hypoxanthine, guanine and xanthine to IMP, GMP and XMP, at 245nm, 257.5nm and 255nm, respectively. The concentration of enzyme (75µg/ml) and

PribPP (100uM) were kept constant. The reaction was carried out at 1.0cm path length at UV Visible spectrometer 1601 (Shimadzu) in the reaction buffer at the room temperature. The initial velocity (V_0 [μM/min]) was calculated using Lambert-Beer law for 7 different concentration of the individual substrate molecules:

$$A=\Delta\varepsilon*L*c$$

where A is measured absorbance, L is length of cuvette, Δε is constatnt (5817$M^{-1}*cm^{-1}$ for guanine, 2283$M^{-1}*cm^{-1}$ for hypoxanthine and 4685$M^{-1}*cm^{-1}$ for xanthine; Keough *et al*, 1998) and finally, c is concentration of the product formed in one minute (V_0). Obtained data were processed with software GraphPad Prism using Michaelis-Menten kinetics to calculate the maximum velocity V_{max} and the Michaelis constant K_m values for individual substrate molecules. K_{cat} was then calculated from the equation:

$$K_{cat}=V_{max}/[E]$$

where [E] is concentration of enzyme.

Specific activity (μmol*s^{-1}*μg^{-1}) of the enzyme is defined as amount of the product (μmol) generated in 1 minute at 60uM purine substrate per 1μg enzyme.

3.4 SDS-PAGE and Western blot

Samples prepared from *T. brucei* whole cell lysates, from *E. coli*, from protein purifications and from digitonin fractionations were heated at 97ºC for 7 minutes, and they were loaded on 12% polyacrylamid gel. For subsequent analysis, the proteins were blotted onto the PVDF membrane (BioRad) incubated over night at PBS-T containing 5% milk. Next day the membranes were incubated with primary antibodies (anti-v5 and anti-His, Invitrogen; anti-enolase and anti-hexokinase, gift from Julius Lukeš, Hannaert *et al.*, 2003, Cárdenas *et al*., 1998; anti-hsp70, anti-XPRT, anti-HGPRT, our own production) for one hour, then they were 3-times washed in PBS-T, incubated with secondary antibodies (anti-mouse and anti-rabbit, BioRad) in milk for one hour followed by another 3-times wash in PBS-T. The signal was visualized using Clarity™ Western ECL Substrate (Biorad) in Chemidoc™ MP instrument (Biorad).

3.5 Sub-cellular fractionation with digitonin

Whole cell lysate was prepared from $1x10^7$ cells expressing TbHGPRT/1_v5 or TbXPRT_v5 proteins. To obtain a membrane and cytosolic fractions, $1x10^8$ cells over-expressing TbHGPRT/1_v5 or TbXPRT_v5 were harvested by centrifugation, washed in

PBS-G, resuspended in 500µl SoTE and lysed with 500µl SoTE containing 0.03% digitonin. The cells were incubated on ice for 5 minutes followed by centrifugation (4ºC, 3000xg, 3 minutes). Supernatant represents the cytosolic fraction (cyto) and pellet represent the membrane fraction (mem).

3.6 Immunofluorescence assay (IFA) to visualize proteins of interest *in situ*

T. brucei cells over-expressing TbHGPRT/1_v5 or TbXPRT_v5 were induced by tetracycline (final concentration 1µg/ml) for 24 hours. $2x10^7$ non-induced cells and $7x10^7$ induced cells were harvested by centrifugation. In a meantime rounded coverslips were treated with 20µl of 10% poly-L-Lysine solution, air-dried and washed 3-times with 1xPBS. The harvested cells were resuspended in 200µl PBS, 40µl cells were added on the coverslip, let it sit for 15 minutes and fixed with 3.6% formaldehyde in 1xPBS for 15 minutes. Then cells were permeabized with 100µl 0.1% Triton X-100 in 1xPBS for 10 minutes followed by 3-times wash with 1xPBS. As a blocking solution, 100µl 5.5% FBS in 1xPBS was added for 45 minutes followed by 2-times washes with 1xPBS. Cells were then incubated for 1 hour with 40µl of 3% BSA in 1xPBS-T containing primary antibodies mouse anti-v5 (1:200), rabbit anti-enolase and rabbit anti-hexokinase (1:200). Primary antibody was washed out using 1xPBS followed by secondary antibodies staining (1:400) goat anti-mouse labeled by Texas Red®-X (Molecular Probes, Invitrogen) or goat anti-rabbit labeled by FITC (Sigma). Cells were washed 3-times with 1xPBS-T and 2-times with 1xPBS. Finally, the coverslips were mounted on a glass slide with VECTASHIELD Mounting media containing DAPI to stain the nucleus and kinetoplast DNA. Coverslips were examined using Yeiss Axioplan 2 microscope (Carl Yeiss, Jena, Germany). Pictures were taken using F-view CCD camera, and photos were colored using Adobe Photoshop.

3.7 Alamar blue assay

All ANPs were tested on wild type BF427 cells, and the most efficient ones were also tested on TbHGPRT/1_v5 over-expressing cells line.

The 96-well plate was filled with 100ul of HMI-9 media. Into the last well of each row, 25ul of the studied compound (25mM) was added and mixed shortly. Out of the last well, 25ul of solution was taken and added into the next well (generating a dilution by 5). The dilution was continued until the last well. By this procedure the drug solution was diluted along the row giving a serial dilution of the drug (Figure 3.4). Then, 100ul of cells

($1x10^4$) were added into an each well (diluting the compound again by 2), resulting in a final cell concentration at $5x10^3$ per well. The plate was left for 24 hours at 37°C, then 20ul of resazu-rine solution (100ug/ml) was added and incubated for additional 6 hours.

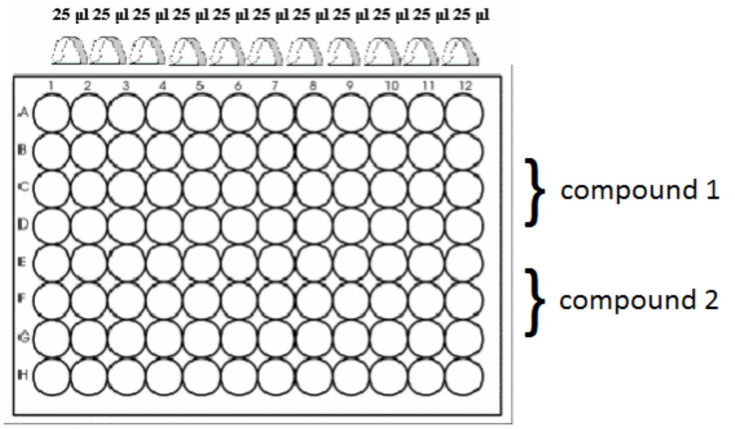

Figure 3.4: Limited dilution scheme.

The resulting fluorescence was read on the microplate reader (TECAN) using fluorescence excitation wavelength of 540-570nm and reading emission at 580-610nm. The results were analyzed by plotting the fluorescence intensity versus compound concentration using nonlineral regression (curve fit) and sigmodial dose-response analysis by Graph Pad Prism software.

3.8 Growth curves

T. brucei RNAi cell lines carrying the p2T7-177/HGPRT+XPRT vector were growing in 5ml in HMI-9/G/Phleo medium. Cells were divided into two different flasks (non-induced and induced) at the concentration of $2x10^5$ cells/ml. RNAi cells were induced by tetracycline (final concentration 1µg/ml). Cell density was measured every day by Beckam Coulter Z2 Particle Counter. If their cell density reached $5x10^5$ cells/ml, the culture was split down to the starting density of $2x10^5$ cells/ml.

3.9 Real-time quantitative PCR

3.9.1 RNA isolation

RNA from single markers, non induced cells and RNAi induced cells for two or four days was purified using RNA blue reagent (TopBio) accordingly to the manufacturer's protocol. Briefly, $7x10^8$ cells were incubated for 10 minutes in RT in 25ml of RNA blue reagent, then 5ml of chloroform was added, tubes were shaken vigorously and were spun down (10 minutes, 12.000xg at 4°C). Upper aqueous phase was transferred to a fresh tube, 12.5ml of isopropanol solution was added and tubes were incubated for 2 hours at 4°C.

Samples were then centrifuged (30 minutes, 12.000xg at 4°C), washed with 10ml of ice-cold 75% ethanol and spun down (10 minutes, 12.000xg at 4°C). The samples were air-dried for 5-10 minutes, the RNA was resuspended in sterile MilliQ/RNAse-free water. Final concentration of RNA samples were determined with Nanodrop (Thermo Scientific).

3.9.2 Reverse transcription, creation of cDNA

Isolated RNA from SM, non induced cells, induced cells (15µg) was treated with Dnase I accordingly to DNA-free kit (Applied Biosystems). Reverse transcription reaction took place in a volume of 20µl accordingly to Transcriptor HF cDNA synthesis kit (Roche; Table 3.3). Reaction without the reverse trascriptase (-RT) enzyme served as a control for DNA contamination. RNA samples with random primers were mixed to reverse transcription (Table 3.4).

Table 3.3: Preparation to reverse trascription.

5x First Strand Buffer	4µl
Protector Rnase Inhibitor	0.5µl
dNTP Mix	2µl
DTT	1µl
RT	1.1µl
MiliQ water	11.5µl

Table 3.4: RNA sample preparation to reverse trascription.

RNA	4µg
Random primers	250ng
MiliQ water	To 11.4µl

RNA samples including random primers (Table 3.4) were first heated at 65°C for 10 minutes and then left on ice for 1 minute. Then the enzyme mixture (Table 3.3) was added to the samples, incubated at 29°C for 10 minute, at 48°C for 60 minutes and 85°C for 5 minutes in the PCR cycler. cDNA was then kept on ice or stored at -20°C. For the purpose of real-time qPCR, RT samples were diluted 500x with water and -RT samples were diluted 10x.

3.9.3 Real-Time qPCR

LC480 Multiwell Plate 96-white well plate (Roche) and LC480 SYBR Green I Master kit were used. 18S rRNA and β tubuline primers served as an internal control. One reaction contained: 10µl 2xSYBR Green I master, 2µl cDNA and 4µl 300nM specific primes (Table 3.5) or 4µl 300nM 18S rRNA primers or 4µl 300nM β tubuline primers. All samples were prepared in triplicates. The reaction plate was run in LightCycler 480 according to the program:

1. denaturation95ºC 10minutes

2. denaturaton 95ºC 15 seconds

3. Annealing 60ºC 1minute

Cycle was repeated 65 times.

Table 3.5: qPCR primers

TbXPRT Fw	CCGGGAGTACCGACCTGCCA
TbXPRT Rv	CGACCACCGGGCTTGTCCAC
TbHGPRT Fw	GTGTGGCGCAGCGTATTGCC
TbHGPRT Rv	GGGCAGCTTCGTCTTCACTGCT

Melting curves were measured to determine a present of single amplicon. Obtained data were analyzed by LightCycler 480 Software, linear regression of PCR efficiency was calculated by LinRegPCR program, and mean efficiency value for every sample was counted using Pfaffle calculation table.

3.10 Solutions and Buffers

Agarose plate:

1% tryton, 0.5% yeast extract, 0.5% NaCl, 1.5% agar

Dialyzing Buffers for TbXPRT_6His:

First buffer: 500mM NaCl, 0.1% sakosyl

Second buffer: 150mM NaCl, 0.1% sakosyl

In vitro Assay Reaction Buffer:

0.1 M Tris-HCL pH 8.5, 0.11M $MgCl_2$

LB medium:

1% tryton, 0.5% yeast extract, 0.5% NaCl

PBS:

5.6mM $Na_2HPO_4x12H_2O$, 3.6mM $NaH_2PO_4x2H_2O$, 0.145M NaCl

PBS-G:

5.6mM $Na_2HPO_4x12H_2O$, 3.6mM $NaH_2PO_4x2H_2O$, 0.145M NaCl, 3.3mM glucose

PBS-T:

5.6mM $Na_2HPO_4x12H_2O$, 3.6mM $NaH_2PO_4x2H_2O$, 0.145M NaCl, 0.05% Tween

Purification Buffer A:

20mM $NaPO_4$ pH 8, 500mM NaCl, 25mM imidazole, 0.2% sarkosyl

Purification Bufffer B:

20mM $NaPO_4$ pH 8, 500mM NaCl, 500mM imidazole, 0.1% sarkosyl

Purification PBS:

20mM $NaPO_4$ pH 8, 500mM NaCl

SDS-PAGE loading dye:

63mM Tris-HCl, 10% glycerol, 2% SDS, 0.0025% Bromophenol Blue, pH 6.8

SOC medium:

2% tryton, 0.5% yeast extract, 10mM NaCl, 2.5mM Kcl, 10mM $MgCl_2$, 10mM $MgSO_4$, 20mM glucose

SoTE:

20mM Tris-HCL pH 7.5, 0.6M sorbitol, 0.4% EDTA

STE:

50mM Tris-HCl, 150mM NaCl, 1mM EDTA

4 Results

4.1 Identification of genes for HGPRT and XPRT in genome of *T. brucei*

HGPRT and XPRT proteins were identified in the genome of *T. brucei* (Kotrbová, 2012; Aistleitner, 2012) using related sequences from *Leishmania donovani* and *L. major* (Jardim *et al*., 1999). TbXPRT is encoded by a single gene (Tb927.10.1390) while TbHGPRT is encoded by two genes (Tb927.10.1400: HGPRT/1, Tb927.10.1470: HGPRT/2). HGPRT/1 and HGPRT/2 are almost identical at the nucleotide and amino acid level (97,6% similarities) with just a few difference at their C-terminus (Fugure 4.1). TbXPRT and TbHGPRT/2 protein sequences contain a glycosomal targeting signal at their C-terminus, and thus these proteins might be localized into the glycosomes. In contrary, TbHGPRT/1 is missing such a signal and its localization could not be predicted using various software.

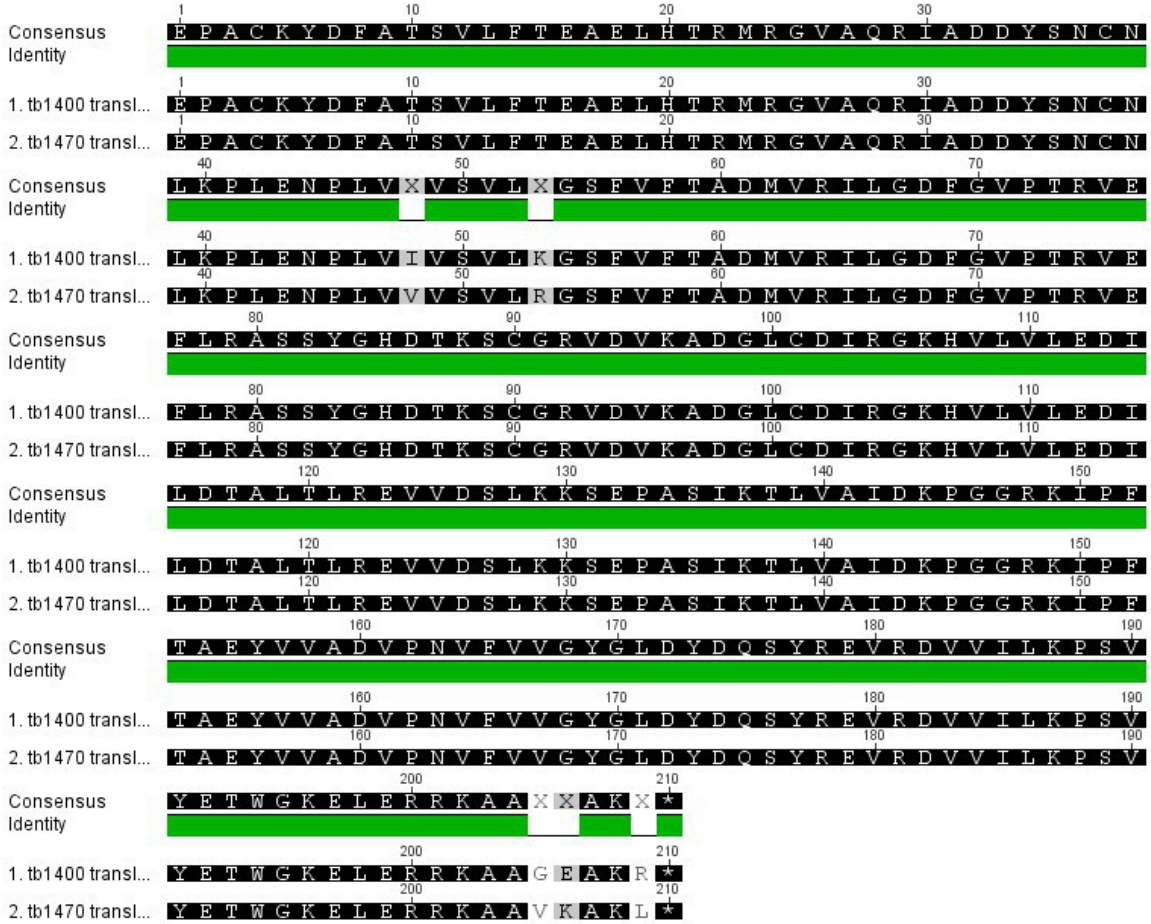

Figure 4.1: Protein sequence alignment of TbHGPRT/1 (Tb1400) and TbHGPRT/2 (Tb1470) in *T. brucei*. Alignment was created using Geneious.

4.2 *In vitro* characterization of TbHGPRT/1_6His and TbXPRT_6His proteins

4.2.1 Expression, solubility and purification of TbHGPRT/1_6His and TbXPRT_6His proteins

To obtain purified recombinant TbHGPRT/1_6His and TbXPRT_6His proteins for subsequent experiments, the *TbHGPRT/1* and *TbXPRT* open reading frames were cloned into the bacterial vector pSKB3. The N-terminally 6-his tagged TbHGPRT/1 and TbXPRT proteins were expressed and their solubility properties were tested using Bug Buster solution (Figure 4.2).

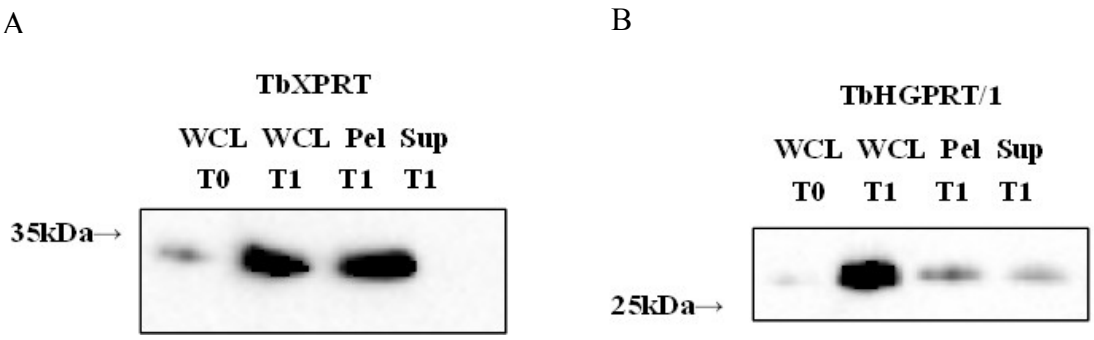

Figure 4.2: Solubility assay with Bug Buster. TbHGPRT/1_6His is half percent soluble, and TbXPRT_6His is insoluble under native conditions.

A: Solubility of TbXPRT_6His

B: Solubility of TbHGPRT/1_6His

Samples from whole cell lysate (WCL) before induction (T0) and later from induction (T1), pellet (Pel) and supernatant (Sup) after treatment with Bug Buster were analyzed by immunoblotting using anti-His (1:1000) primary antibody and anti-mousse (1:1000) secondary antibody.

The recombinant proteins TbHGPRT/1 and TbXPRT were detected using anti-His (Invitrogen) antibody in whole cell lysate after 1 hour of induction (Figure 4.2 A and B). Importantly, the signal for TbHPRT/1_6His was also detected in the soluble fraction (supernatant) suggesting that this protein remains in the cytosol of the bacterial cells and can be purified using native condition. In contrast to these results, the recombinant TbXPRT_6His protein was detected only in the pellet fraction implying that under the conditions used, this protein is assembled into the inclusion bodies.

4.2.1.1 Purification of recombinant TbHGPRT/1_6His

Since the signal for TbHGPRT/1_6His was detected in the soluble fraction, purification under native condition was performed to obtain purified TbHGPRT/1_6His protein. Cells expressing TbHGPRT/1_6His were treated with lysozyme and Dnase I, and supernatant was further proceed for a purification using ÄKTA prime plus. Flow through and elution fractions were collected and verified on the SDS-PAGE gel (Figure 4.3 A). A little bit of protein is detected in the flow through fraction, suggesting that a small portion of the recombinant protein did not bind to the column. High amount of the recombinant TbHGPRT/1_6His protein appeared in the fractions 4 to7. Elution fractions 4-9 were pooled, dialyzed and checked on the SDS-PAGE gel (Figure 4.3 B). A small degradation of the protein of interest was observed. However, majority of the detected protein runs at the expected size.

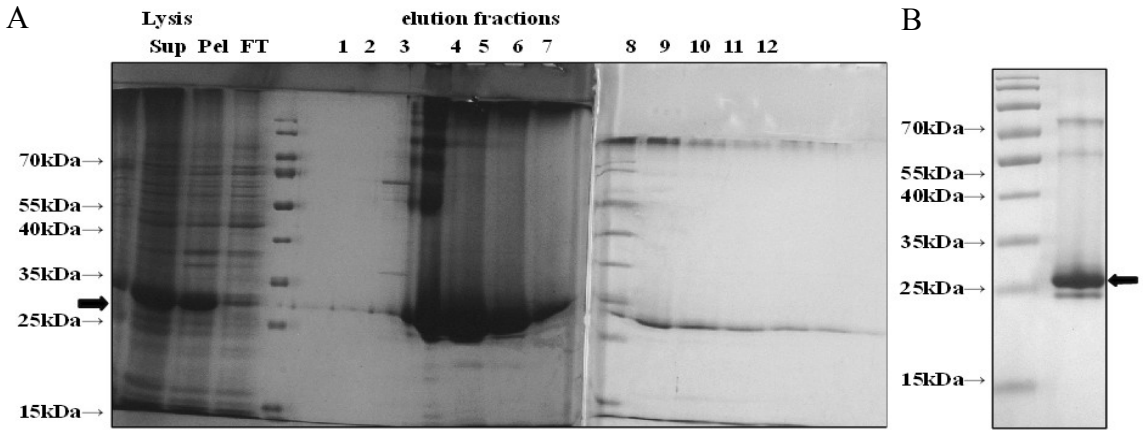

Figure 4.3: Native purification of TbHGPRT/1. TbHGPRT/1 was successfully purified.

A: Purification profile of TbHGPRT/1_6His

B: Verification after dialysis

In every step of purification the samples were taken and verified on the SDS-PAGE gel. Lysis Sup: supernatant after treatment with lysozyme and Dnase I loaded on purification column; Lysis Pel: Pellet after treatment with lysozyme and Dnase I; FT: flow trough; elution fraction 1-12.

Gel was stained by coomasie.

Bradford analysis revealed that 14mg of the recombinant TbHGPRT/1_6His protein was purified. The amount of 2.7mg of the purified protein was sent for an antibody production, and the rest of the protein was kept at -20 and used for *in vitro* assays.

In summary, we purified sufficient amount of the recombinant protein under native condition for a specific antibody production and for *in vitro* assays (see below).

4.2.1.2 Purification of TbXPRT

Unlike TbHGPRT/1_6His, TbXPRT_6His is insoluble and could not be purified under the native condition. Therefore, a detergent sarkosyl was used to solubilize inclusion bodies. Induced *E. coli* cells expressing TbXPRT_6His were treated with lysozyme and Dnase I, and pellet after this lysis was treated with sarkosyl. After the spin, supernatant was diluted to decrease the sarkosyl concentration and loaded on a Ni-NTA column using ÄKTA Prime plus instrument. As in the case of TbHGPRT/1_6His, samples were taken from every step of purification and verified on the SDS-PAGE gel (Figure 4.4).

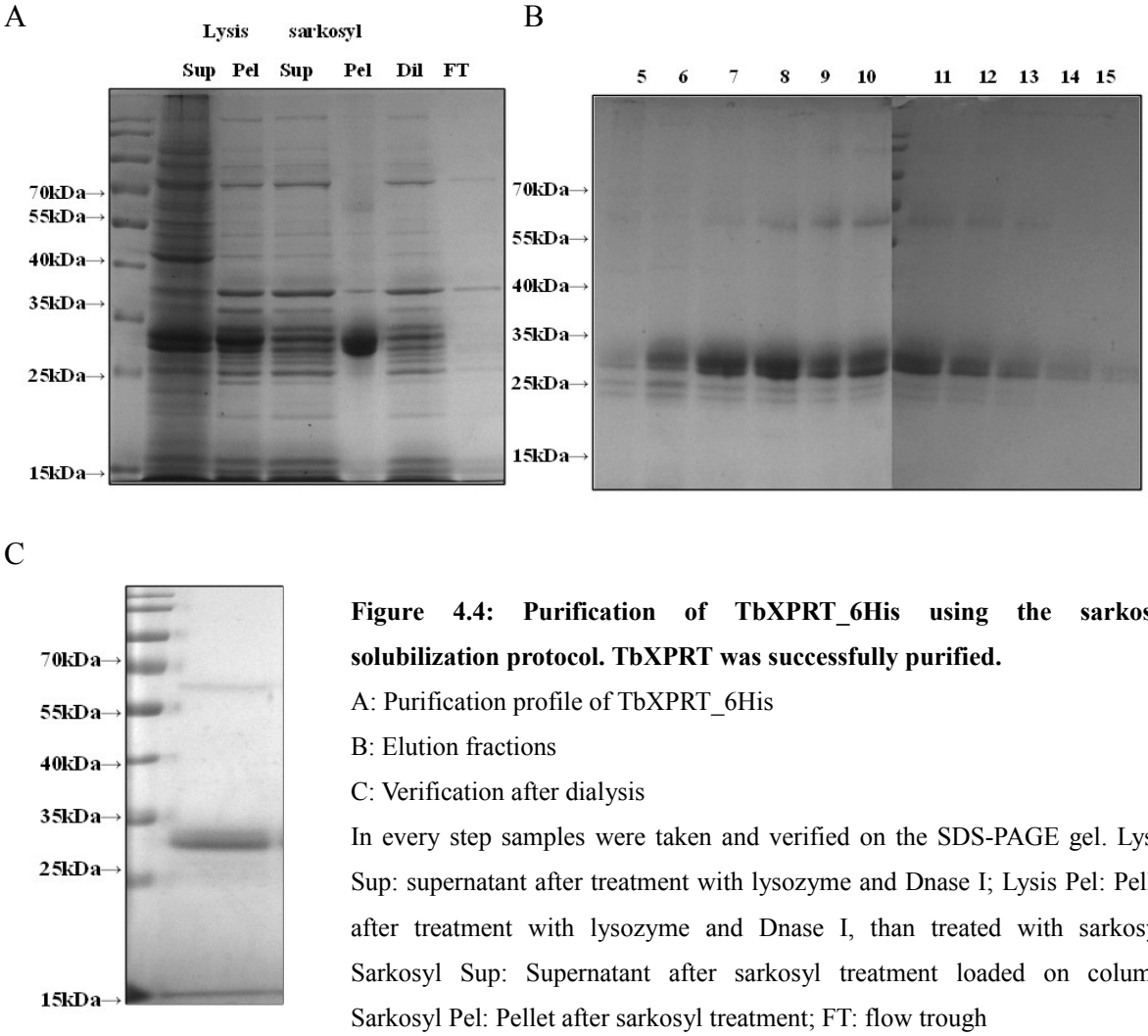

Figure 4.4: Purification of TbXPRT_6His using the sarkosyl solubilization protocol. TbXPRT was successfully purified.

A: Purification profile of TbXPRT_6His

B: Elution fractions

C: Verification after dialysis

In every step samples were taken and verified on the SDS-PAGE gel. Lysis Sup: supernatant after treatment with lysozyme and Dnase I; Lysis Pel: Pellet after treatment with lysozyme and Dnase I, than treated with sarkosyl; Sarkosyl Sup: Supernatant after sarkosyl treatment loaded on column; Sarkosyl Pel: Pellet after sarkosyl treatment; FT: flow trough

Gel was stained by coomasie.

Though most of the protein is detected in the pellet after the treatment with sarkosyl, a sufficient amount of TbXPRT_6His protein stayed in the supernatant and was loaded

on the Ni-NTA column (Figure 4.4 A). Protein of interest appeared in the elution fraction 6 and disappeared in the fraction 12 (Figure 4.4 B). Hence, these fractions were collected and dialyzed. After dialysis, a band of an appropriate size was detected (Figure 4.4 C). Bradford analysis revealed that 1.43mg of recombinant protein was purified. This amount of the protein was sent for an antibody production. In summary, using the sarkosyl solubilization protocol we purified sufficient amount of protein for specific antibody production.

4.2.2 *In vitro* activity of the recombinant TbHGPRT/1_6His protein

Activity of the purified recombinant TbHGPRT/1_6His was measured *in vitro* by spectrophotometry (Figure 4.5 Table 4.1). Values for V_o (µM/min) calculated for different concentration of hypoxanthine and guanine were used. Using steady-state conditions, TbHGPRT/1_6His exhibited a K_m value of 13.23µM for hypoxanthine when PRibPP was fixed at concentration of 30mM and a k_{cat} value of 0.202s^{-1}. Gaunine was also recognized by HGPRT/1_6His protein as substrate with K_m value of 6.35µM and k_{cat} value of 0.184s^{-1}.

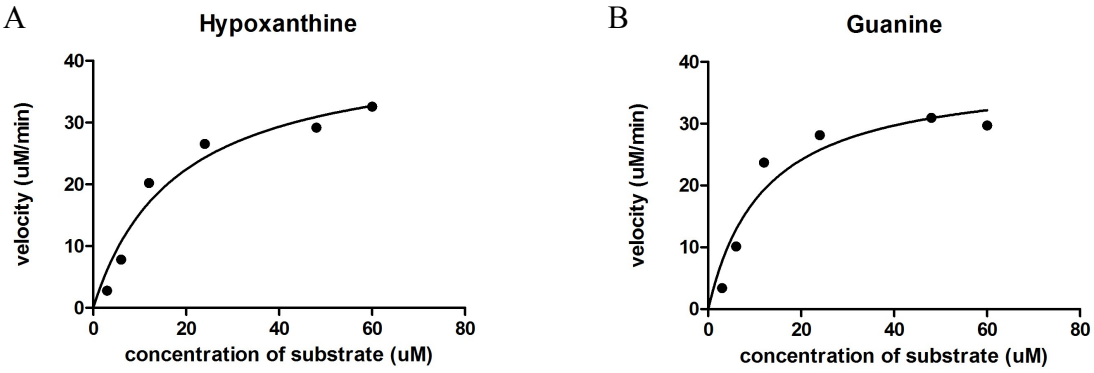

Figure 4.5: Michaelis-Melten kinetics model of recombinant TbHGPRT/1_6His for hypoxanthine (A) and guanine (B).

2.5µM enzyme, 1mM PRibPP and different concentration of purine substrates (hypoxanthine, guanine and xanthine) were used to assay at pH 8.5. The initial velocity was calculated from the change of absorbance that happened during the first 10s reaction, the value was then related to 60 seconds. The dependence of initial velocity on substrate concentration was processed by GraphPad Prism software using Michaelis-Menten kinetics.

Table 4.1: Kinetic constants for TbHGPRT/1_6His and Specific activities.

	Hypoxanthine	Guanine	Xanthine
K_m (µM)	13.3	6.35	Non
V_{max} (µM*s^{-1})	0.607	0.552	Non
K_{cat} (s^{-1})	0.202	0.184	Non
K_{cat}/K_m (µM-^{1}*s^{-1})	0.015	0.029	Non
Specific activities of HGPRT (µmol*s^{-1}*µg-^{1})	0.434	0.396	Non

As predicted by the homology search, recombinant TbHGPRT/1_6His can bind only hypoxanthine and guanine while xanthine was not recognized at all. The catalytic efficiencies for hypoxanthine and guanine are very similar. Nevertheless, conversion of guanine to GMP is slightly more effective than conversion of hypoxanthine to IMP, although V_{max} and K_{cat} are slightly better for hypoxanthine reaction. In summary, we confirmed *in vitro* specificity of recombinant TbHGPRT/1_6His to hypoxanthine and guanine.

Activity of TbXPRT_6His could not be evaluated, because sarkosyl blocked the activity of the enzyme, although we attempted to remove it by dialysis.

4.2.3 Test of specific antibodies against TbXPRT and TbHGPRT

Specific purified rabbit antibodies against TbHGPRT and TbXPRT were tested using Western blot analysis. Whole cell lysate from $1*10^7$ cells of wild types of both procyclic (PF) and bloodstream form (BF) were fractionated on the SDS-PAGE gel, blotted onto PDVF membrane and probed with the antibodies at dilution 1:1000 (Figure 4.6 A). Anti-XPRT detected same level of XPRT protein in both form. Unfortunately, under these conditions no signal was detected when anti-HGPRT antibody was used (data not shown). Thus, dilution of 1:500 (Figure 4.6 B) was tested using the same samples. Using these conditions, a weak band was detected in PF cells while no band was detected in BF lane. The non-purified serum was also tested resulting in a detection of a weak band of expected size also in BF lane in addition to a strong band at ~38Kda. This band most likely represents a cross-reaction with unknown protein (Figure 4.6 C). Moreover, anti-HGPRT antibody was tested on recombinant TbHGPRT/1_6His protein and on TbHGPRT/1_v5 over-expressing *T. brucei* cell line (Figure 4.7) to verify anti-HGPRT specificity to TbHGPRT protein. Anti-HGPRT recognizes the recombinant TbHGPRT/1_6His at concentration of 8,8μg. The expression of v5-tagged TbHGPRT/1_v5 was also recognized by anti-HGPRT antibody, weakly in non-induced cells and strongly in the tet-induced cells (Figure 4.7).

In summary, purified anti-XPRT serum works satisfactory at dilution 1:1000 detecting only one band of the expected size in both PF427 and BF427 cells. Considering that the same amount of cells was loaded on a gel, we can conclude that the level of TbXPRT expression is the same in PF and BF cells. On the other hand, purified anti-HGPRT appeared as a weak antibody recognizing TbHGPRT only in PF cells. When non-purified serum was tested, two bands were detected and the lower band was of the expected size. Comparing the intensity of the TbHGPRT band to the higher band serving as a loading control we can

conclude that TbHGPRT protein seems to be regulated at the expression level between PF and BF cells.

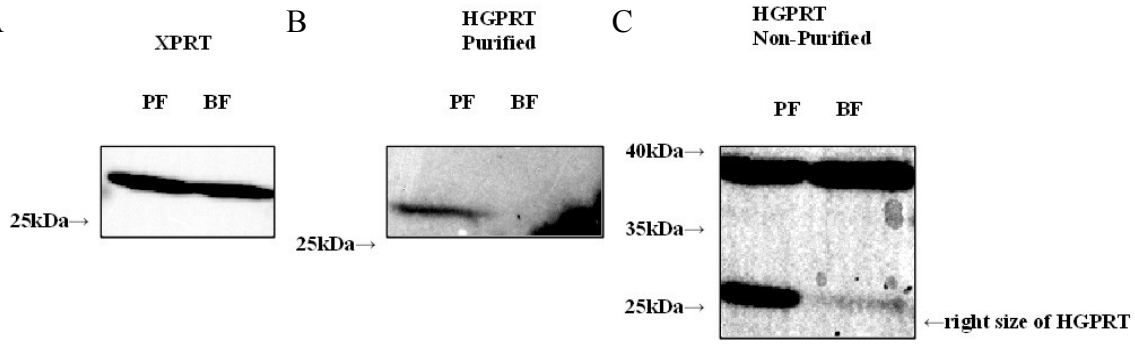

Figure 4.6: Testing of specific antibodies.

A: Purified anti-XPRT; dilution 1:1000

B: Purified anti-HGPRT; dilution 1:500

C: Non-purified anti-HGPRT; dilution 1: 500

$1*10^7$ cells per well of PF or BF were loaded on 12% SDS-PAGE gel, and probed with protein specific primary antibody and anti-rabbit (1:1000) secondary antibody.

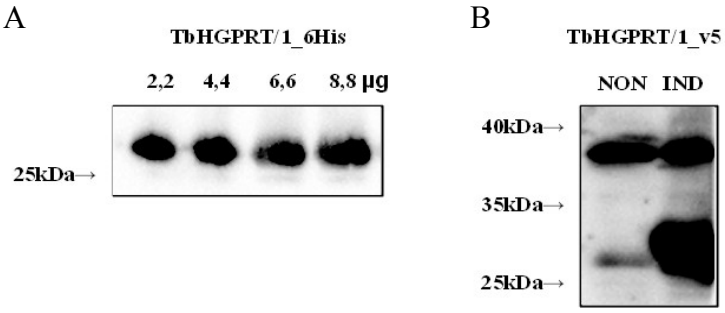

Figure 4.7: Testing of non-purified anti-HGPRT antibody to recombinant TbHGPRT/1_6His (A) and on TbHGPRT/1_v5 over-expressing cell line (B).

A: 2.2, 4.4, 6.6 and 8.8µg recombinant protein was loaded on 12% SDS-PAGE. Non-purified primary anti-HGPRT was diluted 1:250 and anti-rabbit secondary antibody was diluted 1:1000

B: $1*10^7$ cells per well of TbHGPRT/1_v5 over-expressing cell were loaded on 12% SDS-PAGE gel. Lysates were analyzed with non-purified primary anti-HGPRT (1:250) and anti-rabbit secondary antibody (1:1000).

Based on these results, we decided to use purified anti-XPRT at the dilution 1:1000 with the cell lysate made from $1*10^7$ cells per well and non purified anti-HGPRT at the dilution 1:250 with the cell lysate made from $2*10^7$ cells per well to obtain reproducible results. The nonspecific band visible, when anti-HGPRT serum is used, serves as a loading control.

4.3 *In vivo* characterization of TbHGPRT/1_v5 and TbXPRT_v5 proteins

4.3.1 Sub-cellular localization of TbHGPRT/1_v5 and TbXPRT_v5

Sub-cellular localization of TbHGPRT/1, TbHGPRT/2 and TbXPRT was unknown in cells of *T. brucei.* Therefore, we tried to determine localization using two methods: digitonin fractionation and immunofluorescence assay. For both methods a cell line, in which the expression of TbHGPRT/1_v5, TbHGPRT/2_v5 or TbXPRT_v5 tagged protein can be induced by addition of tetracycline into the media, was used. Three for TbXPRT_v5, two for TbHGPRT/1_v5 and one for TbHGPRT/2_v5 cell lines were induced for 48 hours, and the over-expression of the protein of interest was verified by Western blot (Figure 4.8).

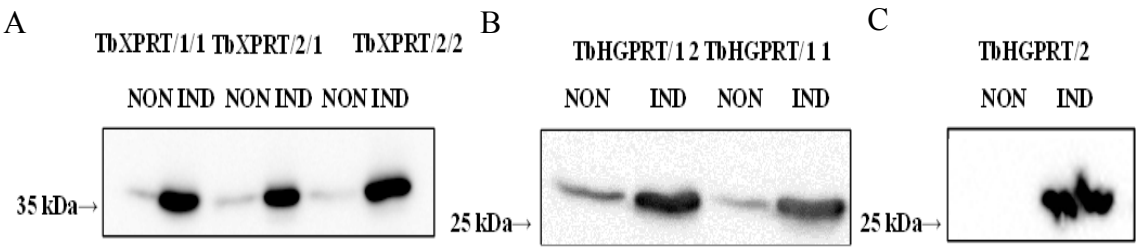

Figure 4.8: Verification of over-expression by Western Blot.

A: Verification of TbXPRT_v5; predicted size 36kDa

B: Verification of TbHGPRT/1_v5; predicted size 28kDa

C: Verification of TbHGPRT/2_v5; predicted size 28kDa

$1*10^7$ cells per well were loaded on 12% SDS-PAGE gel, and probed with anti-v5 (1:1000) primary antibody and anti-mouse (1:1000) secondary antibody.

Western blots suggested, that all proteins are being expressed in all tested cell lines. Importantly, signal was also detected in lanes containing whole cell lysates from non-induced cells, suggesting a leaky expression of protein of interest without tetracycline induction. This phenomena is usually explain by a strong activity of the T7 RNA polymerase and by an uncompleted repressing mechanism by tetracycline repressor protein. For the subsequent analysis, the cell lines TbXPRT_v5/1 and TbHGPRT/1_v5/1 were used. TbHGPRT/2_v5 cell line was not used for following analysis because it had been created very recently and we plan to characterize this cell line in a near future.

4.3.1.1 Sub-cellular fractionation with digitonin

A plant glycoside digitonin is a detergent dissolving fats, especially cholesterol. Hence, it can dissolve cholesterol rich cell membranes in low concentration. Using this method, we were able to separate the membrane fraction from the cytosol, and thus detected the localization of targeted proteins TbXPRT_v5 and TbHGPRT/1_v5 (Figure 4.9).

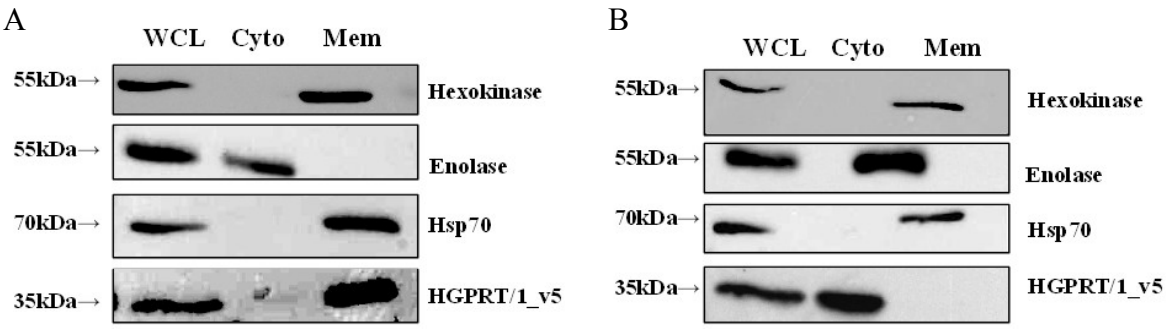

Figure 4.9: Sub-cellular fractionation with digitonin. TbXPRT_v5 is localized into the membrane fraction, and TbHGPRT/1_v5 is localized into the cytosolic fraction.

A: Localization of TbXPRT_v5

B: Localization of TbHGPRT/1_v5

First blot: glycosomal marker hexokinase (50kDa); second blot. cytosolic marker enolase (47kDa); third blot: mitochodrial marker hsp70 (71kDa); fourth blot: target proteins

WCL: whole cell lysate; Cyto: cytosolic fraction; Mem: membrane fraction

$1*10^6$ cells per well were loaded on 12% SDS-PAGE gel, and probed with specific primary antibody and anti-rabbit (1:1000; hexokinase and enolase) and anti-mouse (v5 and hsp70) secondary antibody.

Cells over-expressing TbXPRT_v5 and TbHGPRT/1_v5 proteins were treated with digitonin, and the whole cell, cytosolic and membrane fractions were analyzed using SDS-PAGE followed by Western blot analysis. The TbXPRT_v5 protein was detected in the membrane fraction, the same fraction in which the glycosomal marker hexokinase was present (Figure 4.9 A). On the other hand, TbHGPRT/1_v5 protein was detected in the cytosolic fraction (Figure 4.9 B). The correct localization of marker proteins in the individual fractions verified accuracy of the digitonin treatment. Since this method cannot distinguish between different membrane cellular fractions (glycosomal vs. mitochondrial), immunofluorescence assay (IFA) was performed to distinguish between different cellular compartments.

4.3.1.2 Immunofluorescence assay (IFA)

Using this method, localizations of proteins of interest were performed *in situ* in fixed cells on a slide. The proteins of interest were visualized using a primary antibody against the tag followed by a fluorescent labeled secondary antibody. The cells were then observed under the fluorescence microscope. Pictures were captured using CCD camera and they were further processed in Photoshop program. The known proteins as enolase and hexokinase were used as marker proteins for the cytosol and glycosomes, respectively.

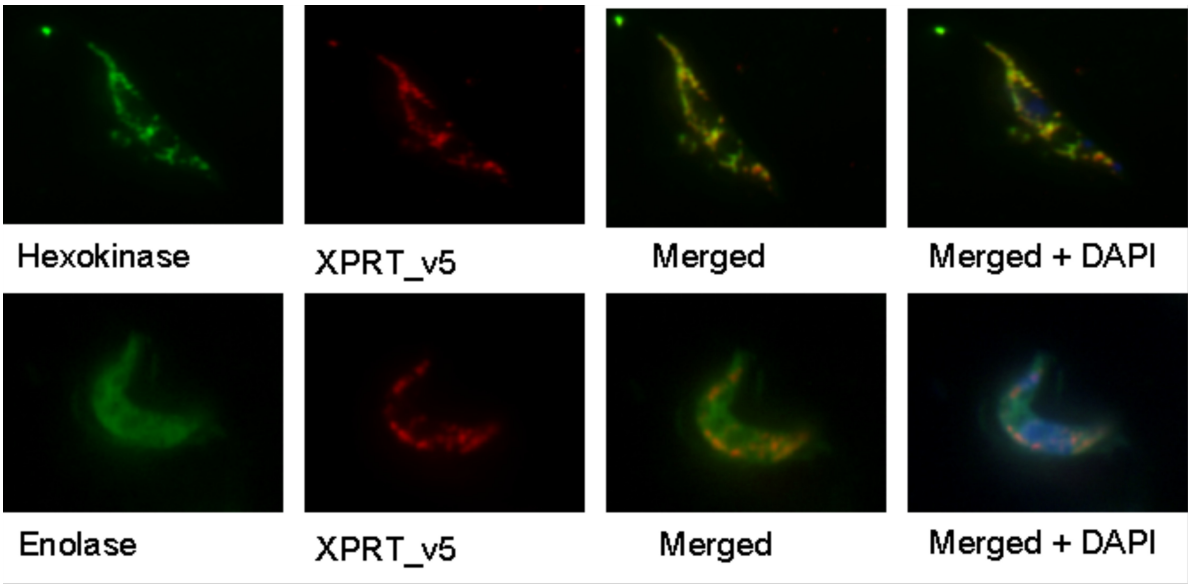

Figure 4.10: TbXPRT_v5 is localized to the glycosome. Hexokinase: glycosomal marker; enolase: cytosolic marker; 4,6-diamino-2-phenylindole (DAPI): staining of nuclear and kinetoplast DNA; merged: fluorescence from hexokinase or enolase with TbXPRT_v5; merged + DAPI: hexokinase or enolase, TbXPRT_v5 and DAPI. The secondary antibody to v5 on target proteins was conjugated with Texas Red®-X (red color), and the secondary antibody to glycosomal and cytosolic markers were labeled with FITC (green color). Organelles containing DNA (nucleus and kinetoplast) are blue. Co-localized proteins in merged picture are orange.

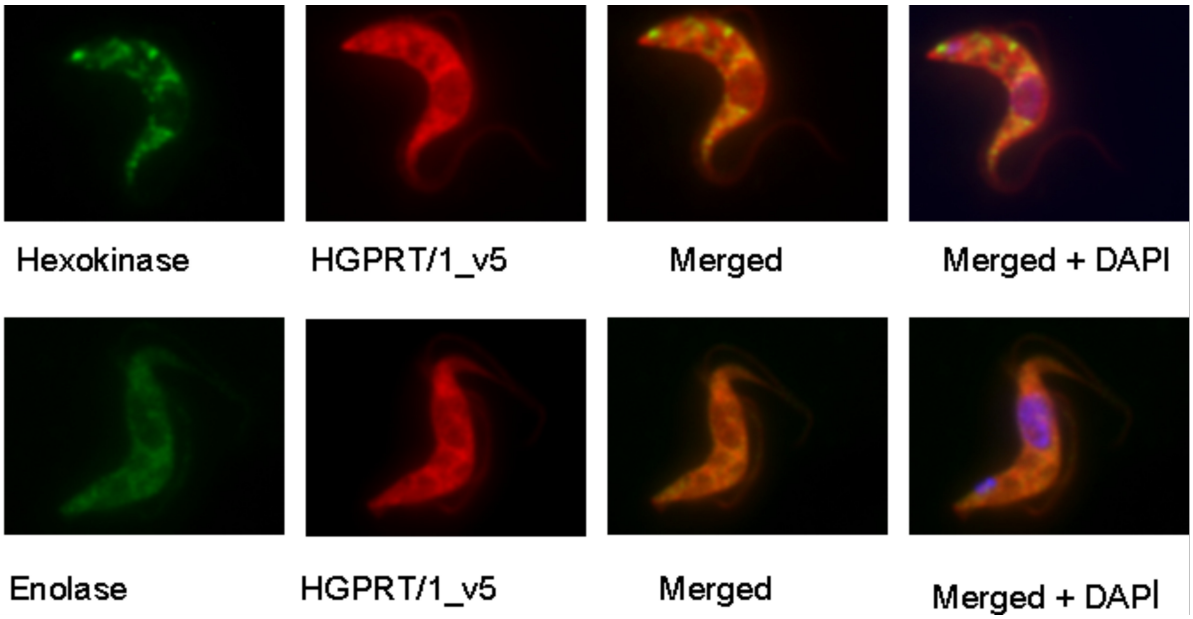

Figure 4.11: TbHGPRT/1_v5 is localized to the cytosol. Hexokinase: glycosomal marker; enolase: cytosolic marker; 4,6-diamino-2-phenylindole (DAPI): staining of nuclear and kinetoplast DNA; merged: fluorescence from hexokinase or enolase with TbHGPRT/1_v5; merged + DAPI: hexokinase or enolase, TbHGPRT/1_v5 and DAPI.

The secondary antibody to v5 on target proteins was conjugated with Texas Red®-X (red color), and the secondary antibody to glycosomal and cytosolic markers were labeled with FITC (green color). Organelles containing DNA (nucleus and kinetoplast) are blue. Co-localized proteins in merged picture are orange.

Our results suggest that TbXPRT_v5 is localized to the glycosomes because the red signal co-localizes with the glycosomal marker hexokinase (Figure 4.10). On the other hand, TbHGPRT/1_v5 seems to be localized to the cytosol because its signal overlaps with the cytosolic marker enolase (Figure 4.11). Moreover, localization of TbXPRT_v5 to glycosomes is supported by a presence of PTS1 at the C-terminal end while TbHGPRT/1_v5 has no such a signal. Importantly, the N-terminal v5-tag did not interfere with the glycosomal import of TbXPRT. In summary, these results confirm localization TbHGPRT/1_v5 into the cytosol and determine localization of TbXPRT_v5 into the glycosomes.

4.3.2 Cytotoxicity of selected ANPs tested in TbHGPRT/1_v5 cell line

The cell proliferation can be measured by an Alamar blue assay (Räz et al., 1997). This method was used to evaluate if some types of ANPs can inhibit the growth of BF *T. brucei* cells. Until now, nearly one hundred of ANPs have been tested in our laboratory and

the most efficient compounds were selected (Table 4.2). To test if these compounds bind to and inhibit TbHGPRT enzyme, compounds containing hypoxanthine or guanine nucleobase were used to estimate IC_{50} values for non-induced cells and cells expressing TbHGPRT/1_v5 protein. We hypothesized that an increase IC_{50} value in induced over-expressing cells in comparison to non-induced would indicate that TbHGPRT is indeed the target for the tested compounds. The parental single marker cell line (SM), non-induced and induced TbHGPRT/1_v5 cell line were incubated with selected ANPs for 24 hours, treated with resazurine for additional 6 hours and the IC_{50} values were calculated using Graph Pad Prism (Table 4.3, Figure 4.12).

Table 4.2: IC50 of efficient ANPs testing on wild types.

Compound	IC50 (µM)
DA-XII-73	0,69
DA-XIII-21	2,995±0,42
PP-P351	1,43±1,09
PP-P364	1,9
DA-XIII-47	5
PP-P369	3,715±2,67
PP-P372	1,53±0,10
PMEG	2,2±0,14
S-HPMPG	3±0,35

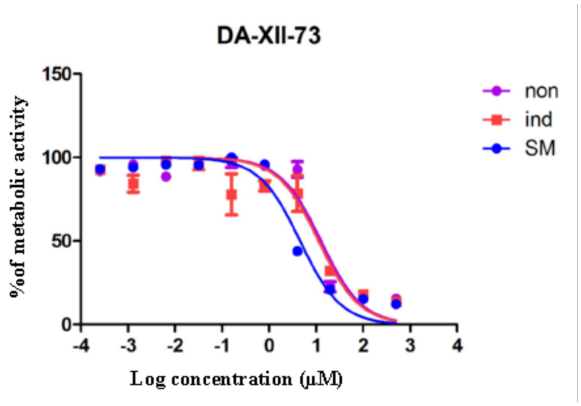

Figure 4.12: Action of one ANP (DA-XII-73) on single markers (SM), induced (ind) and non-induced (non) TbHGPRT/1_v5 over-expressed cell line. Proliferation were evaluated by Alamar blue assay. These data were processed with GraphPad Prism using non-lineral regression.

Table 4.3: IC50 of efficient ANPs for single markers (SM), non-induced (NON) and induced (IND) TbHGPRT/1_v5 over-expressed cells. Experiment was repeated several times and the average IC50 values with its standard deviations are calculated.

Compound	**IC50 (µM)** SM	**IC50 (µM)** NON(HGPRT/1_v5)	**IC50 (µM)** IND(HGPRT/1_v5)
DA-XII-73	5,4±1,26	13,1±0,42	16,7±6,74
DA-XIII-47	9,49±3,71	15,08±5,91	18,38±2,02
PP-P369	5,99±0,27	11,91±2,16	17,59±3,01
PP-P351	4,47±0,75	6,35±0,71	13,25±1,06

As expected, the IC_{50} values for the selected 4 compounds were in low micromolar values. When IC50 values were compared between non-induced and induced cells, no significant differences were found. However, when these values were compared to SM cells, the IC50 values for non-induced and induced cells were up to 3 times higher than the IC50 values determined for SM cells. These results can be explained by a leakage expression of TbHGPRT/1_v5 tagged protein in non-induced cells as it is apparent from the Figure 4.8. In this figure, the non-induced cells showed a background expression of the tagged TbHGPRT enzyme which may have an effect on IC_{50} values measured in this cell line. In summary, these results suggest that the selected ANPs may inhibit the TbHGPRT enzyme.

4.3.3 Silencing expression of TbXPRT and TbHGPRT by RNAi

To determine, if TbHGPRT and TbXPRT are essential, the expression of these two genes was silenced by RNAi.

4.3.3.1 Analysis of growth phenotype in single knock-down (SKD) cell lines

In the past, no growth phenotype was detected in single knock-down (SKD) RNAi lines silencing expression of TbXPRT or TbHGPRT in regular HMI-9 media containing hypoxanthine as a major purine source (Figure 4.13 A for XPRT; Figure 4.14 A for HGPRT; Aistleitner, 2012). These results might be explained by two views. First, when TbHGPRT is silenced then TbXPRT has an affinity to hypoxanthine and can convert this molecule to IMP. Second, regular fetal bowing serum (FBS) containing purine molecules, was used in this experiment. Due to this fact, the growth of cells can be rescued by the purines obtained from FBS. To evaluate a growth of SKD RNAi cell line, we prepared media that contains only one type of purine source (hypoxanthine or xanthine) and used dialyzed fetal bovine serum (Invitrogen).

In the case of SKD TbXPRT RNAi cells, a strong growth phenotype was observed second day after RNAi induction in the medium containing only xanthine (Figure 4.13 B). Therefore, we concluded that TbHGPRT cannot convert xanthine to XMP, and xanthine is modified only by TbXPRT. In the medium with hypoxanthine, no growth phenotype was observed for SKD TbXPRT RNAi cells confirming the activity of TbHGPRT that converts hypoxanthine to IMP (Figure 4.13 C).

A

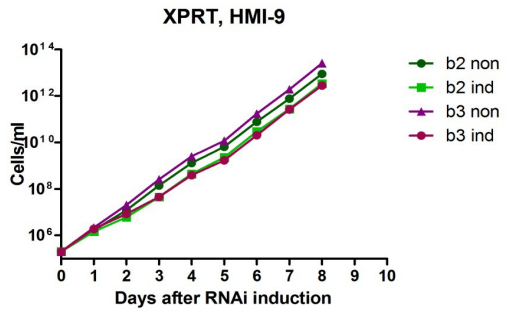

B

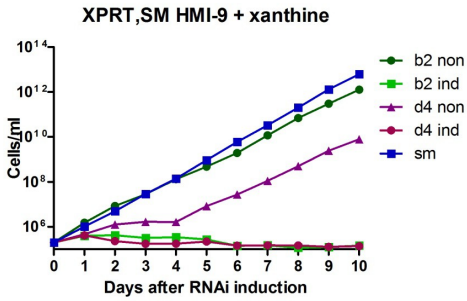

C

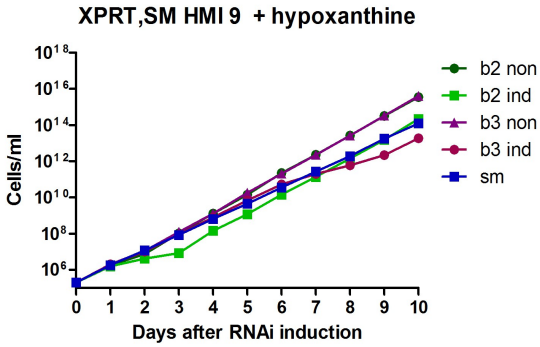

Figure 4.13: Growth phenotype of SKD TbXPRT RNAi. In HMI-9 with xanthine TbXPRT is essential for bloodstream form of *T. brucei*.

A: Regular HMI-9 (Data from Martina Aistleitner)

B: HMI-9 with 50µM xanthine

C: HMI-9 with 50µM hypoxanthine

Both non-induced (non) and induced (ind) cell lines were diluted if they reached concentration more than $5x10^5$ cell/ml and were growing in 5 ml of media. Single markers (SM) served as a control.

A

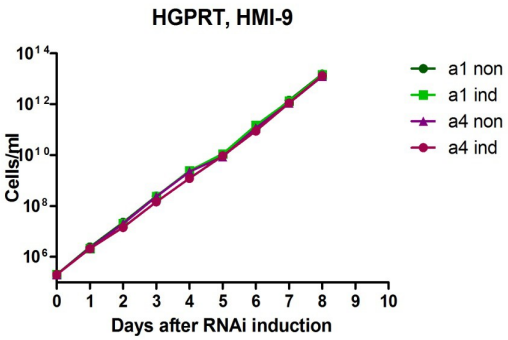

B

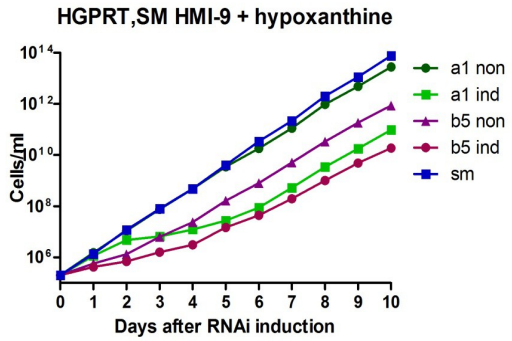

C

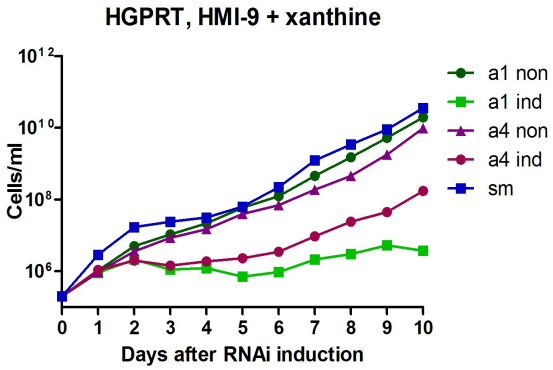

Figure 4.14: Growth phenotype of SKD TbHGPRT RNAi. In HMI-9 with hypoxanthine slightly phenotype was observed.

A: Regular HMI-9 (Data from Martina Aistleitner)

B: HMI-9 with 50µM hypoxanthine

C: HMI-9 with 50µM xanthine

Both non-induced (non) and induced (ind) cell lines were diluted if they reached concentration more than $5x10^5$ cell/ml and were growing in 5 ml of media. Single markers (SM) served as a control.

In the case of SKD TbHGPRT RNAi cells, a mild growth phenotype was detected third day after RNAi induction in the medium containing hypoxanthine. After 4 days of RNAi induction, the induced cells reached similar doubling time as non-induced, suggesting an adaptation to the growth conditions. These data may suggest, that TbXPRT can also act on hypoxanthine, and after few day of growth only in hypoxanthine environment TbXPRT was able to fully substitute TbHGPRT. Parental cell line SM and SKD TbHGPRT cells were grown in the media, containing xanthine as the only purine source. Since xanthine is the least preferable source of purines in *T. brucei*, the growth of SM and non-induced cells was mildly affected. Interestingly, a strong phenotype was observed when RNAi was induced, suggesting that TbXPRT was not able to function properly. This observation is difficult to explain and currently the cell line is being verified for RNAi specificity.

Taking all these data together, it seems, that TbXPRT is more promiscuous than TbHGPRT and can act on both hypoxanthine and xanthine. In contrast, TbHGPRT can act only on hypoxanthine. It should be noted that guanine was not tested in these assays.

4.3.3.2 Analysis of growth phenotype in double knock-down (DKD) cell lines

Because RNAi induced silencing expression had not led to a growth phenotype in regular HMI-9, double knock-down (DKD) TbHGPRT/TbXPRT RNAi cell line was created. Non-induced and induced DKD TbHGPRT/TbXPRT RNAi cell lines were growing in regular HMI-9, and their density was measured every day (Figure 4.15).

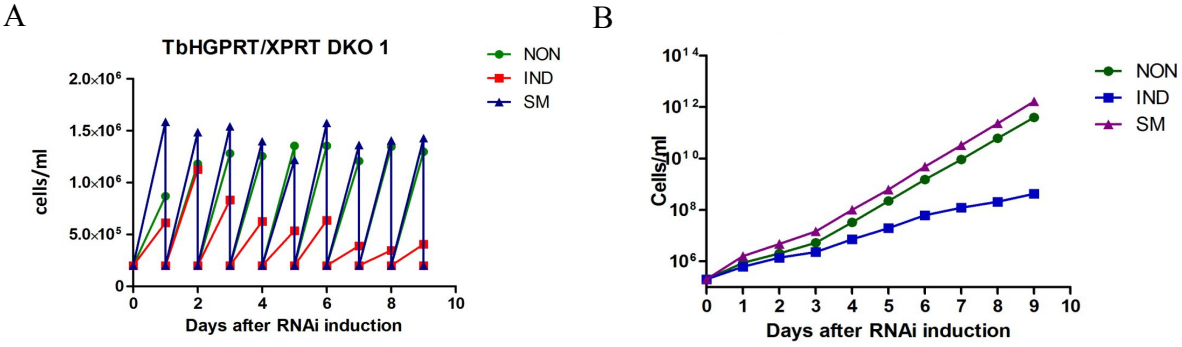

Figure 4.15: Growth phenotype of DKD TbHGPRT/TbXPRT RNAi cell lines. Both genes are essential for bloodstream form of *T. brucei*.

A: Non cumulative model of graph

B: Cumulative model of graph

Both non-induced (NON) and induced (IND) cell lines were diluted every day to concentration $2x10^5$ cell/ml and were growing in 5 ml of media. Single markers (SM) served as a control.

The growth curve shows a growth phenotype after three days upon RNAi induction. However, as in the case of SKD cell lines, phenotype was not strong as expected, likely because of purines coming from regular FBS. Due to this fact, DKD TbHGPRT/TbXPRT cells were examined in HMI-9 with dialyzed FBS and with defined purine sources like hypoxanthine, xanthine and adenosine (Figure 4.16).

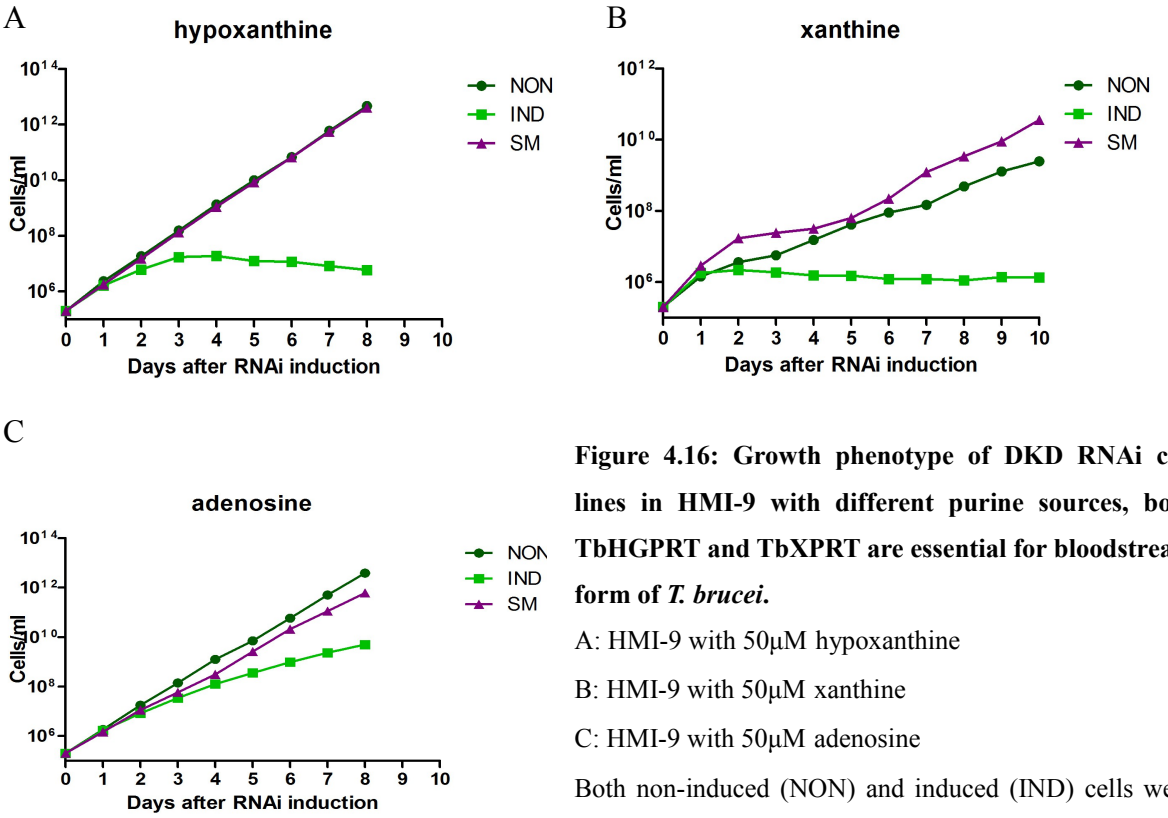

Figure 4.16: Growth phenotype of DKD RNAi cell lines in HMI-9 with different purine sources, both TbHGPRT and TbXPRT are essential for bloodstream form of *T. brucei*.

A: HMI-9 with 50µM hypoxanthine

B: HMI-9 with 50µM xanthine

C: HMI-9 with 50µM adenosine

Both non-induced (NON) and induced (IND) cells were diluted if they reached concentration more than $5x10^5$ cell/ml and were growing in 5 ml of media. Single markers (SM) served as a control.

Importantly, strong growth phenotypes were observed in media containing hypoxanthine or xanthine. These results imply that TbHGPRT and TbXPRT are essential for bloodstream form of *T. brucei*, and their insufficient activity leads to the stagnation in growth. These results suggest that TbHGPRT and TbXPRT are the only enzymes that can convert nucleobase to its monophosphate analog. When both genes are silenced, the cells are not able to divide when 6-oxopurines are in the media.

Interestingly, a mild growth phenotype was observed in the medium containing adenosine. This result was not expected since *T. brucei* possess a strong adenosine kinase activity and several active adenosine transporters (Berg *et al.*, 2010). However it seems plausible that when the cells are grown in the regular HMI-9 media containing hypoxanthine

that cells may lose the immediate ability to salvage adenosine. Because of this fact, the DKD TbHGPRT/TbXPRT cells were grown in the medium containing adenosine for two weeks to adapt, and after this time the RNAi experiment was repeated (Figure 4.17).

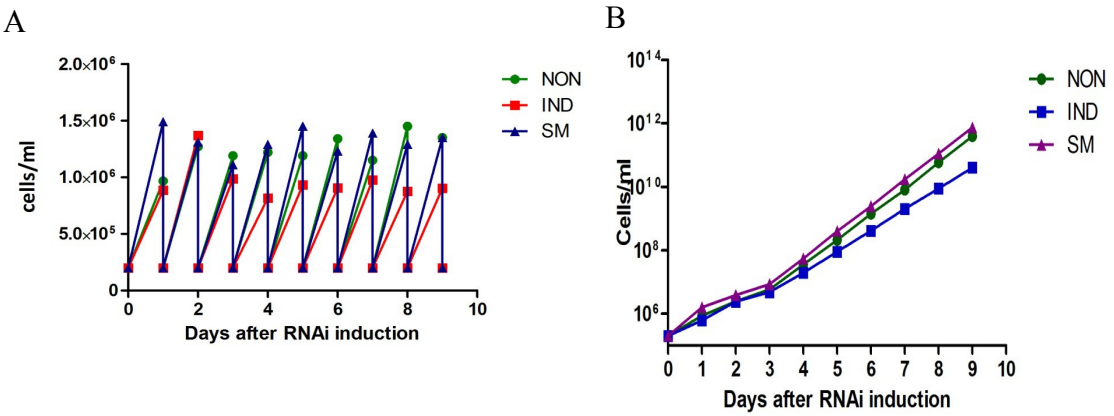

Figure 4.17: Growth phenotype of DKD TbHGPRT/TbXPRT RNAi cell lines in HMI-9 with 50µM adenosine. Adenosine rescue cells.

A: Non cumulative model of graph

B: Cumulative model of graph

Both non-induced (NON) and induced (IND) cells were diluted every day to concentration $2x10^5$ cell/ml and were growing in 5 ml of media. Single markers (SM) served as a control.

Due to adenosine preincubation, the RNAi induced growth phenotype observed in the previous experiment was almost diminished. Accordingly to this result, cells of *T. brucei* sufficiently adapted to adenosine as a sole purine source after two weeks.

4.3.3.3 Verifying of silencing expression

RNA interference was verified by qPCR (DKD cell lines) and by specific anti-XPRT antibody.

4.3.3.3.1 Verifying of silencing expression by qPCR

Decreased levels of TbHGPRT and TbXPRT mRNA in DKD TbHGPRT/TbXPRT RNAi cell line were quantified by real-time quantitative PCR (Figure 4.18).

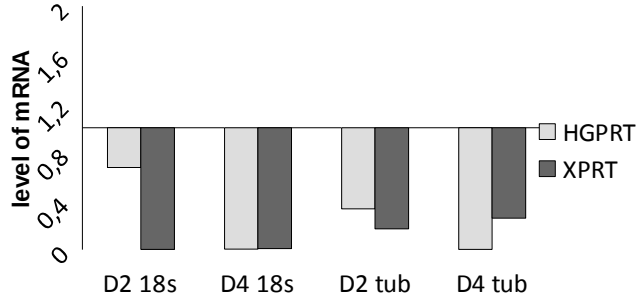

Figure 4.18: Real-time quantitative PCR verified silencing expression both TbHGPRT and TbXPRT in DKD TbHGPRT/TbXPRT RNAi cell line.

The RNA levels were measured in triplicates and were normalized to 18s rRNA (18s) and β tubuline (tub). cDNA serving as a template was created from RNA collected before induction and after two (D4) or four (D4) days and induction.

qPCR showed a significant decrease in expression of both *TbHGPRT* and *TbXPRT* genes. These results confirmed silencing expression of both TbHGPRT and TbXPRT in DKD TbHGPRT/TbXPRT RNAi cell line.

4.3.3.3.2 Verifying of silencing expression by specific anti-XPRT antibody

Moreover, regulation of expression in SKD TbXPRT, SKD TbHGPRT and DKD TbXPRT/TbHGPRT RNAi lines was verified by Western blot using anti-XPRT primary antibody (Figure 4.19)

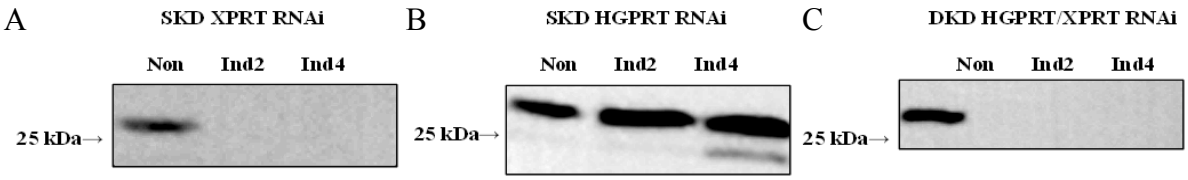

Figure 4.19: Anti-XPRT antibody confirmed decreasing level of TbXPRT in a SKD TbXPRT RNAi and in a DKD TbHGPRT/TbXPRT RNAi cell lines.

$1x10^7$ non induced cells (Non); induced cells for 2 (Ind2) or 4 days (Ind4) were loaded onto the 12% SDS-PAGE gel and blotted to PDVF membrane. Lysates were analyzed with anti-XPRT (1:1000) primary antibody and anti-rabbit (1:1000) secondary antibody.

Anti-XPRT detected a decrease in TbXPRT protein level in SKD TbXPRT (Figure 4.19 A) and DKD TbHGPRT/TbXPRT RNAi cell lines (Figure 4.19 C) while in SKD TbHGPRT RNAi protein level was unaffected (Figure 4.19 B). This result confirms efficient RNAi silencing of TbXPRT expression in both SKD TbXPRT RNAi and DKD TbHGPRT/TbXPRT RNAi cell lines. Anti-HGPRT was not used to verify these RNAi lines because of its low recognition level.

5 Discussion and conclusion

5.1 *In vitro* characterization of TbHGPRT/1

Recombinant TbHGPRT/1_6His and TbXPRT_6His proteins were purified and sent to produce specific antibodies. TbHGPRT/1_6His was purified under the native condition, and its activity was measured in *in vitro* assay. Unfortunately, TbXPRT_6His was purified with the detergent called sarkosyl, which blocks the activity of the enzyme even after a thorough dialysis. A purification under denaturing conditions with 8M urea with subsequent refolding did not yield in sufficient amount of protein for the *in vitro* activity assay. Therefore, a careful optimization of the purification protocols is needed to obtain sufficient amount of the TbXPRT_6His protein for *in vitro* assay.

The TbHGPRT/1_6His activity was characterized *in vitro* using the protocol developed for *Plasmodium* cells (Keough *et al*., 1998). We showed that recombinant TbHGPRT/1_6His is active, and hypoxanthine and guanine act as substrates molecules with similar efficiency. K_m and K_{cat} values acquired for *T. brucei* TbHGPRT/1_6His were compared to human HGPRT, *Plasmodium* HGXPRT, *Leishmania* HGPRT and XPRT and *E. coli* XGPRT and HPRT (Table 5.1).

The most effective 6-oxopurine PRT is *E. coli* XGPRT, because its K_{cat} values are the highest. Moreover, the efficient constant K_{cat}/K_m of *E. coli* XGPRT for guanine is up to 10-time higher than efficient constants for other enzymes and substrates. According to our result, HGPRT of *T. brucei* is 60-times less active than HGPRT of *L. donovani* and 300-less active than HGXPRT of *P. falciparum* when the efficiency constant were compared. The observed low efficiency constant might be be reasoned by several observation.: First, the recombinant TbHGPRT/1_6His was stored for one month in -20ºC and during this time this enzyme was several times thawed and refrozen which could result in lower activity. Second, concentrations of purines can be different among various cells due to the activity of purines transporters. *T. brucei* might posses more active transporters, so the concentration of purines inside *T. brucei* cell might be higher than in *L. donovani* or *P. falciparum* cell. For example adenosine concentration in mammalian blood is less than 0.01µM (Gruber *et al*., 1989; Moser *et al.*, 1989) while in *T. brucei* it varies between 1.2-1.8µM due to activity of adenosine transporters depending on the log growth phase as adenosine transporters are expressed less during the early growth phase compared to the later growth phase. (Graven *et al.*, 2014).Therefore, there is a possibility that concentration of hypoxanthine and guanine

might be considerably greater in *T. brucei* then in blood. Third, unlike *T. brucei*, *P. falciparum* and *L. donovani* are intracellular parasites, and so the concentration of purines might be higher than in the bloodstream. For instance mammalian plasma contains hypoxanthine at concentration of ~2,5µM while erythrocyte's cytoplasm contains hypoxanthine at concentration of ~ 8µM (Boulieu *et al*., 1983).

Table 5.1: Kinetic constant for *T. brucei*, Human, *Plasmodium*, *Leishmania* and *E. coli* 6-oxopurine PRTases.

Organism	Substrate	K_m (µM)	K_{cat} (s^{-1})	K_{cat}/K_m ($\mu M^{-1}*s^{-1}$)
***T. brucei* HGPRT**	Hypoxanthine	13.23	0.202	0.015
	Guanine	6.35	0.184	0.029
	Xanthine	Non	Non	Non
Human HGPRT[a]	Hypoxanthine	3.4±1	5.2±0.4	1.5
	Guanine	1.9±0.4	8.2±0.6	4.3
	Xanthine	Non	Non	Non
***P. falciparum* HGXPRT[a]**	Hypoxanthine	0.07±0.03	0.33±0.08	4.3
	Guanine	0.83±0.5	0.66±0.07	0.8
	Xanthine	189±18	3.3±0.2	0.02
***L. donovani* HGPRT[b]**	Hypoxanthine	6.4	5.7	0.89
	Guanine	9.9	12.1	1.23
	Xanthine	Non	Non	Non
***L. donovani* XPRT[c]**	Hypoxanthine	448±97	2.6±0.2	0.006
	Guanine	>100	0,003	Non
	Xanthine	7.1±2.3	3.5±1.5	0.49
***E. coli* XGPRT[a]**	Hypoxanthine	90.8±11.3	13.7±1.3	0.02
	Guanine	2.6±0.7	34.1±2.7	13.1
	Xanthine	30.5±2.6	37.5±0.7	1.2
***E. coli* HPRT[a]**	Hypoxanthine	12.5±2.4	59±3.5	4.9
	Guanine	294±20	10.2±0,7	0.03
	Xanthine	45.9±2.5	0.008±0.001	0.0003

[a] Keough *et al.*, 2010; [b] Allen *et al.*, 1995; [c] Jardim *et al*., 1999

T brucei HGPRT has similar trend of the specific activity in comparison to *L. donovani* HGPRT. Both HGPRTases have similar specific activity to hypoxanthine and guanine and cannot convert xanthine (Allen *et al*., 1995). *L. donovani* XPRT prefers xanthine as a main substrate. However, it can transform with lower efficacy also hypoxanthine (Jardim *et al*., 1999). Similar preferences might be found also in *T. brucei* XPRT, as the SKD HGPRT cell lines was able to growth on hypoxanthine. Therefore, it is

very important to purify recombinant TbXPRT_6His without sarkosyl and perform *in vitro* assays to evaluate specific activity of *T. brucei* XPRT.

5.2 Sub-cellular localization

The predicted localizations of TbXPRT and TbHGPRT/1 were verified by experimental procedures. Both digitonin fractionation and immunofluorescence analysis showed that TbXPRT_v5 is localized into the glycosomes while TbHGPRT/1_v5 is localized into the cytosol. Moreover, the localization of TbXPRT_v5 to glycosomes is supported by the presence of PTS1 C-terminal signal. In contrast, TbHGPRT/1 C-terminal ends with the AKR sequence that has never be predicted as glycosomal targeting signal (Shih *et al*., 1998). In the past, we used C-terminal v5-tagging for TbHGPRT and TbXPRT, showing that this tag interferes with the PTS1 of TbXPRT as this protein was found in the cytosol (Kotrbová, 2012). Due to transfection problems, analysis of TbHGPRT/2 localization has not been performed yet. However, we predict that TbHGPRT/2 will be localized into the glycosomes because it contains the glycosomal targeting signal PTS1. Moreover, TbHGPRT/2 was identified in the glycosomal fraction in the past (Colasante *et al*., 2006). Importantly, in Colasante's study the TbHGPRT/2 protein was found in the glycosomes of the procyclic form while it was not detected in the bloodstream form. The absence of signal for HGPRT/2 protein in the glycosomal fraction of BF cells can be explained by its down regulation of expression in this stage (Vertommen *et al.*, 2008). Therefore, it is important to experimentally show localization of TbHGPRT/2 in the bloodstream form to support the bioinformatic prediction. Further, it would be interesting to check expression of TbHGPRT/1 and TbHGPRT/2 in procyclic and bloodstream form because there is a possibility that one form of TbHGPRT is more expressed in the bloodstream form and the second from TbHGPRT is expressed in the procyclic form.

HGPRT and XPRT enzymes were extensively studied in cells of *L. donovani*, where they were localized into glycosomes using several techniques: confocal microscopy, fluorescent microscopy (Shih *et al*., 1998), and localization of XPRT was also confirmed with sub-cellular fractionation (Zarella-Boitz *et al.*, 2004). Moreover, creating an *L. donovani* mutant with XPRT without PTS1 verified importance of PTS1 in the glycosomal transport, because this XPRT cannot cross glycosomal membrane and remained in the cytosol. Nevertheless, PTS1 in XPRT is not essential for its function, as XPRT without PTS1 was stable and was active (Zarella-Boitz *et al.*, 2004). Thus, cytosolic localization of *T. brucei* HGPRT/1 may have no effect on its function.

5.3 Effect of selected ANPs on cells of *T. brucei*

Next aim of this study was to determine IC50 values for several compounds from the class of acyclic nucleoside phosphonates to evaluate their potential as chemotherapeutic. In cooperation with the laboratory of Zlatko Janeba (UOCHB, Prague), we screened nearly one hundred of these compounds. Nine of the selected ANPs with hypoxanthine or guanine in their structure were found to be effictive in micro and nano molar concentration. These are DA-XIII-47, DA-XIII-21, PP-P351, PP-P364, PP-P369, PP-P372, PMEG and S-HPMPG. A few selected compounds which we have in sufficient quantity, were tested on TbHGPRT/1_v5 over-expressing cell lines and on the parental cell line. A significant difference in IC50 values was detected between the parental cell line and induced cells. Almost no difference was detected between non-induced and induced cells. This result might be explained by a leaky transcription of TbHGPRT/1_v5 protein in non-induced cells by T7 RNA polymerase even in the absence of tetracycline. Such expression was visible on the western analysis investigating the level of Tb HGPRT/1_v5 in non-induced and induced cells. DA-XII-73 was the most effective compound, since its IC50 value for the parental cell line was 3-time lower than for TbHGPRT/1_v5 over-expressed induced cells. These data are in accordance with result from *Plasmodium*, where the IC50 of the most effective compounds were in range 1-10μM (Česnek *et al*., 2012).

Accordingly to this data, new more effective compounds are being synthesized in the laboratory of Zlatko Janeba. In future, we would like to analyze more compounds especially with xanthine in their structure, because these might efficiently inhibit TbXPRT. In addition, a combination of two different ANPs might generate higher inhibitory effect in the BF cells. Moreover, *in vitro* study of the inhibiting properties of ANPs using TbHGPRT/1_6His protein is in progress. It might be very interesting to define K_m for these compounds. Furthermore, K_i values for similar ANPs compounds were determined for human HGPRT in a frame of the *Plasmodium* project, and these K_i are considerably greater, suggesting that these compounds do not affect the human enzyme (Hocková *et al.*, 2012).

5.4 Importance of XPRT and HGPRT for *T. brucei* BF cells

The single-knock downs of TbHGPRT or TbXPRT have no effect on *T. brucei* bloodstream form. On the other hand, it has been shown using the double-knock down that TbHGPRT and TbXPRT are essential for *T. brucei* bloodstream form. Therefore, these results suggest similarities in the enzyme activity of these two enzymes. This observation

confirms the versatily of PSP (Berg et al., 2010a). Moreover, our result are in agreement with the studies on *L. donovani* cells, where single-knock downs did not result in growth phenotype while the double-knock out was lethal (Boitz and Ullman, 2006a; Boitz and Ullman, 2006b).

To investigate the exact role of the studied enzymes we examined SKD TbXPRT, SKD TbHGPRT and DKD TbXPRT/TbHGPRT RNAi cell lines in the media containing just one type of a purine molecule. Thus, we find out that TbXPRT is essential for *T. brucei* under the conditions, when xanthine is the only purine source. In this way, the activity of TbHGPRT cannot support the cell growth in the media with only xanthine as purine source suggesting that TbHGPRT cannot convert xanthine to its monophosphate nucleotide. This result is in agreement with our *in vitro* study which showed no TbHGPRT activity with xanthine as a substrate. On the other hand, when TbHGPRT expression is silenced by RNAi, TbXPRT can compensate the activity of TbHGPRT, because almost no phenotype was detected in the media containing hypoxanthine as the only purine source. Because it seems that TbXPRT can act on hypoxanthine, it is necessary to develop new purification protocol to TbXPRT_6His to confirm these results *in vitro*. Surprisingly, a strong growth phenotype was observed for TbHGPRT RNAi cells in the medium with xanthine. In this case TbXPRT should be able to utilize xanthine creating XMP and sustain the PSP. It is noteworthy that xanthine is the least preferred purine source, and if xanthine is the only source cells are growing very slowly. In the future, it would be interesting to investigate if the cell can adapt to only xanthine conditions, and if the activity and abundance of the XPRT enzyme would not be sufficient to support the growth of RNAi TbHGPRT cells then.

As expected, the double-knock down TbHGPRT/TbXPRT RNAi cell line exerts a growth phenotype under hypoxanthine or xanthine conditions and leads to cell death. On the other hand, adenosine has the ability to rescue the RNAi cells, thought the cells needed two weeks of adaption to adenosine. This result may suggest that *in vitro* grown *T. brucei* cells are used to utilize hypoxanthine as a typical component of HMI-9 media. Once they are in the media containing only adenosine, the cell metabolism has to adapt to new conditions by higher expression of adenosine transporters, higher expression of adenosine kinase and other PSP enzymes, which are involved in adenosine/adenine salvage. It is possible that adenosine not-adapted cells use pathway through adenosine deaminase to convert adenosine to inosine, followed by activity of IAG-NH to create hypoxanthine and finally the HGPRT enzyme to converts hypoxanthine to IMP. When cells can efficiently

uptake adenosine after a few weeks of incubation, this molecule can be transformed by IAG-NH to adenine and converted to AMP by APRT or can be directly converted to AMP by adenosine kinase (Figure 5.1).

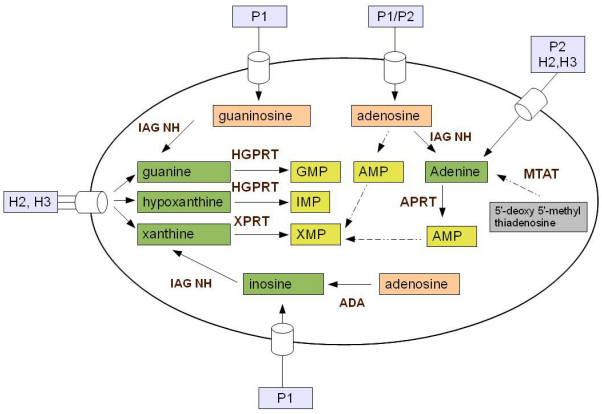

Figure 5.1: Purine salvage pathway in *T. brucei*.

Finally, we confirmed the theory that hypoxanthine and adenosine are more preferred purine sources (Berg *et al.*, 2010a), because doubling time is the shortest for adenosine and hypoxanthine. Nevertheless, cells prefer all purine sources because in regular media containing non-dialyzed serum the doubling time is the shortest (Table 5.2).

Table 5.2: Wild type doubling time in media with different purine source.

	Hypoxanthine	Adenosine	Xanthine	Regular media
Doubling time (hours)	8	9	20	6

5.5 Specific antibodies anti-XPRT and anti-HGPRT

We produced specific antibodies anti-XPRT and anti-HGPRT proteins. Anti-XPRT appears to be an efficient antibody, and it was used to verify the SKD TbXPRT and DKD TbHGPRT/TbXPRT RNAi cell lines. On the other hand, antibody against TbHGPRT seems to be weaker antibody recognizing TbHGPRT only in procyclic cells under low titer conditions. Therefore, we are not able to confirm SKD TbHGPRT and DKD TbXPRT/TbHGPRT RNAi cells with anti-HGPRT. Nevertheless, we showed that anti-HGPRT has affinity to TbHGPRT using recombinant TbHGPRT/1_6His and TbHGPRT/1_v5 cell lines. Thus an absence of the signal for HGPRT in BF cells might be due to low expression of this enzymes in the infectious stage of *T. brucei*.

We showed that TbXPRT seems to be expressed in same level at both BF and PF, whereas TbHGPRT seem to be upregulated in PF compared to BF. In past it was determined that glycosomal TbHGPRT is more concentrated in PF than in BF (Vertommen *et al.*, 2008). Furthermore, TbXPRT was expressed several times more than glycosomal TbHGPRT in bloodstream form of *T. brucei* (Vertommen *et al.*, 2008).

6 Literature

1 Abdelwahab, N. Z., A. T. Crossman, et al. (2012). "Inhibitors incorporating zinc-binding groups target the GlcNAc-PI de-N-acetylase in Trypanosoma brucei, the causative agent of African sleeping sickness." Chem Biol Drug Des **79**(3): 270-278.

2 Allen, T. E., H. Y. Hwang, et al. (1995). "Cloning and expression of the hypoxanthine-guanine phosphoribosyltransferase from leishmania-donovani." Molecular and Biochemical Parasitology **73**(1-2): 133-143.

3 Aistleitner, M. (2012). "Cytotoxicity screen of the acyclic nucleoside phosphonates against bloodstream stage of Trypanosoma brucei and validation of their putative target hypoxanthine/xanthine/guanine phosphoribosyltransferase" Bachelor thesis

4 Berg, M., L. Kohl, et al. (2010). "Evaluation of nucleoside hydrolase inhibitors for treatment of African trypanosomiasis." Antimicrob Agents Chemother **54**(5): 1900-1908.

5 Berg, M., P. Van der Veken, et al. (2010). "Inhibitors of the purine salvage pathway: a valuable approach for antiprotozoal chemotherapy?" Curr Med Chem **17**(23): 2456-2481.

6 Berriman, M., E. Ghedin, et al. (2005). "The genome of the African trypanosome Trypanosoma brucei." Science **309**(5733): 416-422.

7 Boitz, J. M. and B. Ullman (2006). "A conditional mutant deficient in hypoxanthine-guanine phosphoribosyltransferase and xanthine phosphoribosyltransferase validates the purine salvage pathway of Leishmania donovani." J Biol Chem **281**(23): 16084-16089.

8 Boitz, J. M. and B. Ullman (2006). "Leishmania donovani singly deficient in HGPRT, APRT or XPRT are viable in vitro and within mammalian macrophages." Mol Biochem Parasitol **148**(1): 24-30.

9 Boulieu, R., C. Bory, et al. (1983). "Hypoxanthine and xanthine levels determined by high-performance liquid-chromatography in plasma, erythrocyte, and urine samples from healthy-subjects - the problem of hypoxanthine level evolution as a function of time." Analytical Biochemistry **129**(2): 398-404.

10 Brennand, A., D. J. Rigden, et al. (2012). "Trypanosomes contain two highly different isoforms of peroxin PEX13 involved in glycosome biogenesis." FEBS Lett **586**(13): 1765-1771.

11 Cardenas, M. L., A. Cornish-Bowden, et al. (1998). "Evolution and regulatory role of the hexokinase." Biochimica Et Biophysica Acta-Molecular Cell Research **1401**(3): 242-264.

12 Cesnek, M., D. Hockova, et al. (2012). "Synthesis of 9-phosphonoalkyl and 9-phosphonoalkoxyalkyl purines: evaluation of their ability to act as inhibitors of Plasmodium falciparum, Plasmodium vivax and human hypoxanthine-guanine-(xanthine) phosphoribosyltransferases." Bioorg Med Chem **20**(2): 1076-1089.

13 Colasante, C., M. Ellis, et al. (2006). "Comparative proteomics of glycosomes from bloodstream form and procyclic culture form Trypanosoma brucei brucei." Proteomics **6**(11): 3275-3293.

14 Croft, S. L., M. P. Barrett, et al. (2005). "Chemotherapy of trypanosomiases and leishmaniasis." Trends Parasitol **21**(11): 508-512.

15 Dawson, P. A., R. B. Gordon, et al. (2005). "Normal HPRT coding region in a male with gout due to HPRT deficiency." Molecular Genetics and Metabolism **85**(1): 78-80

16 de Clerq, E. (2012). "Highlights in Antiviral Drug Research: Antiviral at the Horizont." Medical Research Rewiews **33**(6): 1215-1248

17 de Clerq, E. (2013). "The Acyclic Nucleoside Phosphonates (ANPs): Antonín Holý's Legacy." Medical Research Rewiews **33**(6): 1278-1303

18 de Jersey, J., A. Holy, et al. (2011). "6-oxopurine phosphoribosyltransferase: a target for the development of antimalarial drugs." Curr Top Med Chem **11**(16): 2085-2102.

19 de Koning, H. P., D. J. Bridges, et al. (2005). "Purine and pyrimidine transport in pathogenic protozoa: From biology to therapy." FEMS Microbiol Rev **29**(5): 987-1020.

20 de Koning, H. P. and S. M. Jarvis (1997). "Purine nucleobase transport in bloodstream forms of Trypanosoma brucei is mediated by two novel transporters." Mol Biochem Parasitol **89**(2): 245-258.

21 Eads, J. C., G. Scapin, et al. (1994). "The crystal-structure of human hypoxanthine-guanine phosphoribosyltransferase with bound gmp." Cell **78**(2): 325-334.

22 Flaspohler, J. A., B. C. Jensen, et al. (2010). "A Novel Protein Kinase Localized to Lipid Droplets Is Required for Droplet Biogenesis in Trypanosomes." Eukaryotic Cell **9**(11): 1702-1710.

23 Freeman, S. and J. M. Gardiner (1996). "Acyclic nucleosides as antiviral compounds." Molecular Biotechnology **5**(2): 125-137.

24 Graven, P., M. Tambalo, et al. (2014). "Purine metabolite and energy charge analysis of Trypanosoma brucei cells in different growth phases using an optimized ion-pair RP-HPLC/UV for the quantification of adenine and guanine pool." Experimental parazitolog **141**: 28-38

25 Gruber, H. E., M. E. Hoffer, et al. (1989). "Increased adenosine concentration in blood from ischemic myocardium by aica riboside - effects on flow, granulocytes, and injury." Circulation **80**(5): 1400-1411.

26 Gualdron-Lopez, M. and P. A. M. Michels (2013). "Processing of the glycosomal matrix-protein import receptor PEX5 of Trypanosoma brucei." Biochemical and Biophysical Research Communications **431**(1): 98-103.

27 Hannaert, V., M. A. Albert, et al. (2003). "Kinetic characterization, structure modelling studies and crystallization of Trypanosoma brucei enolase." Eur J Biochem **270**(15): 3205-3213.

28 Hirumi, H., S. Martin, et al. (1997). "Short communication: cultivation of bloodstream forms of Trypanosoma brucei and T. evansi in a serum-free medium." Trop Med Int Health **2**: 240-244

29 Hockova, D., D. T. Keough, et al. (2012). "Synthesis of novel N-branched acyclic nucleoside phosphonates as potent and selective inhibitors of human, Plasmodium falciparum and Plasmodium vivax 6-oxopurine phosphoribosyltransferases." J Med Chem **55**(13): 6209-6223.

30 Holy, A. (2005). "Synthesis of acyclic nucleoside phosphonates." Curr Protoc Nucleic Acid Chem **14**: Unit 14.12.

31 Hwang, H. Y. and B. Ullman (1997). "Genetic analysis of purine metabolism in Leishmania donovani." J Biol Chem **272**(31): 19488-19496.

32 Chen, S. F., D. H. Shin, et al. (2004). "Crystal structure of methenyltetrahydrofolate synthetase from Mycoplasma pneumoniae (GI : 13508087) at 2.2 angstrom resolution." Proteins-Structure Function and Bioinformatics **56**(4): 839-843.

33 Jardim, A., S. E. Bergeson, et al. (1999). "Xanthine phosphoribosyltransferase from Leishmania donovani. Molecular cloning, biochemical characterization, and genetic analysis." J Biol Chem **274**(48): 34403-34410.

34 Kaminsky, R., B. Nickel, et al. (1998). "Arrest of Trypanosoma brucei rhodesiense and T-brucei brucei in the S-phase of the cell cycle by (S)-9-(3-hydroxy-2-phosphonylmethoxypropyl)adenine ((S)-HPMPA)." Molecular and Biochemical Parasitology **93**(1): 91-100.

35 Kaminsky, R., C. Schmid, et al. (1996). "(S)-9-(3-hydroxy-2-phosphonylmethoxypropyl)adenine (S)-HPMPA : A purine analogue with trypanocidal activity in vitro and in vivo." Tropical Medicine & International Health **1**(2): 255-263.

36 Keough, D. T., D. Hockova, et al. (2009). "Inhibition of hypoxanthine-guanine phosphoribosyltransferase by acyclic nucleoside phosphonates: a new class of antimalarial therapeutics." J Med Chem **52**(14): 4391-4399.

37 Keough, D. T., D. Hockova, et al. (2010). "Plasmodium vivax hypoxanthine-guanine phosphoribosyltransferase: a target for anti-malarial chemotherapy." Mol Biochem Parasitol **173**(2): 165-169.

38 Keough, D. T., A. L. Ng, et al. (1998). Expression and properties of recombinant P-falciparum hypoxanthine-guanine phosphoribosyltransferase. Purine and Pyrimidine Metabolism in Man Ix. A. Griesmacher, P. Chiba and M. M. Muller. New York, Plenum Press Div Plenum Publishing Corp. **431:** 735-739.

39 Kotrbová, Z. (2012). "Ověření působení fosfonátů acyklických nukleosidů na fosforybozyl transferázy 6-oxo purinů u Trypanosomy brucei" Bachelor thesis

40 Krahn, J. M., J. H. Kim, et al. (1997). "Coupled formation of an amidotransferase interdomain ammonia channel and a phosphoribosyltransferase active site." Biochemistry **36**(37): 11061-11068.

41 Lawton, P. (2005). "Purine analogues as antiparasitic agents." Expert Opinion on Therapeutic Patents **15**(8): 987-994.

42 Maser, P., C. Sutterlin, et al. (1999). "A nucleoside transporter from Trypanosoma brucei involved in drug resistance." Science **285**(5425): 242-244.

43 Matthews, K. R. (2005). "The developmental cell biology of Trypanosoma brucei (vol 118, pg 283, 2005)." Journal of Cell Science **118**(9): 2078-2078.

44 Matthews, K. R., J. R. Ellis, et al. (2004). "Molecular regulation of the life cycle of African trypanosomes." Trends in Parasitology **20**(1): 40-47.

45 McCulloch, R. (2004). "Antigenic variation in African trypanosomes: monitoring progress." Trends in Parasitology **20**(3): 117-121.

46 Michels, P. A., F. Bringaud, et al. (2006). "Metabolic functions of glycosomes in trypanosomatids." Biochim Biophys Acta **1763**(12): 1463-1477.

47 Ortiz, D., M. A. Sanchez, et al. (2009). "Two novel nucleobase/pentamidine transporters from Trypanosoma brucei." Mol Biochem Parasitol **163**(2): 67-76.

48 Parkin, D. W. (1996). "Purine-specific nucleoside N-ribohydrolase from Trypanosoma brucei brucei. Purification, specificity, and kinetic mechanism." J Biol Chem **271**(36): 21713-21719.

49 Pays, E., L. Vanhamme, et al. (2004). "Antigenic variation in Trypanosoma brucei: facts, challenges and mysteries." Current Opinion in Microbiology **7**(4): 369-374.

50 Pelle, R., V. L. Schramm, et al. (1998). "Molecular cloning and expression of a purine-specific N-ribohydrolase from Trypanosoma brucei brucei. Sequence, expression, and molecular analysis." J Biol Chem **273**(4): 2118-2126.

51 Penha, L. L., C. B. Sant'Anna, et al. (2009). "Sorting of phosphoglucomutase to glycosomes in Trypanosoma cruzi is mediated by an internal domain." Glycobiology **19**(12): 1462-1472.

52 Räz, B., M. Iten, et al. (1997). "The Alamar Blue assay to determine drug sensitivity od African trypanosomes (T.b. rhodesiense and T.b. gambiense) in vitro." Acta Trop. **68**:139-147.

53 Reyes, P., P. K. Rathod, et al. (1982). "Enzymes of purine and pyrimidine metabolism from the human malaria, Plasmodium-falciparum." Molecular and Biochemical Parasitology **5**(5): 275-290.

54 Sanchez, M. A., R. Tryon, et al. (2002). "Six related nucleoside/nucleobase transporters from Trypanosoma brucei exhibit distinct biochemical functions." Journal of Biological Chemistry **277**(24): 21499-21504.

55 Shih, S., H. Y. Hwang, et al. (1998). "Localization and targeting of the Leishmania donovani hypoxanthine-guanine phosphoribosyltransferase to the glycosome." J Biol Chem **273**(3): 1534-1541.

56 Smeijsters, L., F. F. J. Franssen, et al. (1999). "Inhibition of the in vitro growth of Plasmodium falciparum by acyclic nucleoside phosphonates." International Journal of Antimicrobial Agents **12**(1): 53-61.

57 Schmidt, G. D. and L. S. Roberts, (2009) *Foundations of Parasitology*. McGraw-Hill Companies, New York.

58 Vandemeulebroucke, A., C. Minici, et al. (2010). "Structure and Mechanism of the 6-Oxopurine Nucleosidase from Trypanosoma brucei brucei." Biochemistry **49**(41): 8999-9010.

59 Versees, W., K. Decanniere, et al. (2001). "Structure and function of a novel purine specific nucleoside hydrolase from Trypanosoma vivax." J Mol Biol **307**(5): 1363-1379.

60 Vertommen, D., J. Van Roy, et al. (2008). "Differential expression of glycosomal and mitochondrial proteins in the two major life-cycle stages of Trypanosoma brucei." Mol Biochem Parasitol **158**(2): 189-201.

61 Vodnala, M., A. Fijolek, et al. (2008). "Adenosine kinase mediates high affinity adenosine salvage in Trypanosoma brucei." J Biol Chem **283**(9): 5380-5388.

62 Volf, P., P. Horák et al. (2007) "Paraziti a jejich biologie." Triton

63 Wickstead, B., K. Ersfeld, et al. (2002). "Targeting of a tetracycline-inducible expression system to the transcriptionally silent minichromosomes of Trypanosoma brucei." Mol Biochem Parasitol **125**(1-2): 211-216.

64 Zarella-Boitz, J. M., N. Rager, et al. (2004). "Subcellular localization of adenine and xanthine phosphoribosyltransferases in Leishmania donovani." Mol Biochem Parasitol **134**(1): 43-51.

65 Zhao, Y., Q. Wang, et al. (2012). "Identification of Trypanosoma brucei leucyl-tRNA synthetase inhibitors by pharmacophore- and docking-based virtual screening and synthesis." Bioorg Med Chem **20**(3): 1240-1250.

7 List of abbreviation

ADA:	adenosien deaminase
AK:	adenosine kinase
ANP:	acyclic nucleoside phosphonate
APRT:	adnosine phosphoribosyltransferase
BF:	bloodstream form
cDNA:	complementary DNA
DKD:	double-knock down
dsRNA:	double-straind RNA
FBS:	fetal bowing serum
G:	neomycin
HGPRT:	hypoxanthine-guanine phosphoribosyltransferase
HPRT:	hypoxanthine phosphoribosyltransferase
HGXPRT:	hypoxanthine-guanine-xanthine phosphoribosyltransferase
IAG-NH:	inosine-adenosine-guanosine nucleoside hydrolase
IC50:	inhibitor concentration killing 50% parasites
IG-NH:	inosine-guanosine nucleoside hydrolase
IMP:	inositol monophosphate
MTAP:	methylthioadenine phosphorylase
NH:	nucleoside hydrolase
PCR:	polymerse chain reaction
PF:	procyclic form
Phleo:	phelomycin
PNP:	nucleoside phosphorylase
PRT:	phosphoribosyltransferase
PSP:	purine salvage pathway
PTS:	peroxisomal-targeting signal
PTS1:	C-terminal peroxisomal-targeting signal
PTS2:	N-terminal peroxisomal-targeting signal
Puro:	puromycin
qPCR:	quantitative real time polymerse chain reaction
rDNA:	ribosomal DNA
RNAi:	RNA interfernce

RT:	room temperature
RT:	reverse trasription
SKD:	sinlge knock down
SM:	single markers
VSG coat:	variant surface glycoprotein coat
WCL:	whole cell lysate
XGPRT:	xanthine-guanine phosphoribosyltransferase
XPRT:	xanthine phosphoribosyltransferase